

ETD Archive

2013

Computational Study of Savonius Wind Turbine

Asmita C. Chinchore
Cleveland State University

Follow this and additional works at: <https://engagedscholarship.csuohio.edu/etdarchive>



Part of the [Mechanical Engineering Commons](#)

How does access to this work benefit you? Let us know!

Recommended Citation

Chinchore, Asmita C., "Computational Study of Savonius Wind Turbine" (2013). *ETD Archive*. 852.
<https://engagedscholarship.csuohio.edu/etdarchive/852>

This Thesis is brought to you for free and open access by EngagedScholarship@CSU. It has been accepted for inclusion in ETD Archive by an authorized administrator of EngagedScholarship@CSU. For more information, please contact library.es@csuohio.edu.

COMPUTATIONAL STUDY OF SAVONIUS WIND TURBINE

ASMITA C. CHINCHORE

BACHELOR OF MECHANICAL ENGINEERING

UNIVERSITY OF PUNE INDIA

SPRING 2011

*Submitted in partial fulfillment of requirements for the
degree*

MASTER OF SCIENCE IN MECHANICAL ENGINEERING

at the

CLEVELAND STATE UNIVERSITY

FALL 2013

We hereby approve this thesis of

ASMITA C. CHINCHORE

Candidate for the Master of Science in Mechanical Engineering degree for the

Department of Mechanical Engineering

and the CLEVELAND STATE UNIVERSITY

College of Graduate Studies

Thesis Committee Chairperson, Dr. Majid Rashidi

Department and Date

Dr. Rama S. R. Gorla

Department and Date

Dr Asuquo B. Ebiana

Department and Date

Student's Date of Defense: 12/13/2013

ACKNOWLEDGEMENT

First and foremost, I would like to thank God for his continued support over the last couple of years. I He has truly given me strength and kept me safe and healthy in a whole new country (USA). I am honored to be given the opportunity to positively contribute to the betterment of his world.

Secondly, I would like to thank my advisor Dr. Majid Rashidi, without whose support this thesis could not have been completed. He not only encouraged and challenged me thorough my academic career but also provided proper guidance and reassurance. In spite of his achievements, comprehensive experience and knowledge in the field of engineering design he has always given his students the room to work in their own way. I could not have imagined having a better advisor and mentor for my Master's Study. I would also like to extend my thankfulness to the committee members for giving me their valued time.

I am thankful to all individuals that have supported my efforts, but I would like to pay special thanks to the people that have been very supportive and involved in this thesis and my life on daily basis. With that being said, I would like to specially thank my best friends Chaitanya Lomte and Sonal Boraste for boosting my moral at times when needed and sustaining through all the ups and downs. Additionally, I would like to extend my gratitude to my lab mate Abhinav Gupta, for providing me all the required information and helping me consistently to achieve my results.

I believe that practical engineering research projects that blend state-of-the-art fields of study, software, and innovative design concepts/ideas will continue to pioneer the future of this universe. It is for this reason that I would like to give special thanks to Cleveland State University's Fenn College of Engineering for its commitment to continuing education through its research oriented Grant Program.

Last but not the least; I would like to thank my family: my parents Chandrashekar Chinchore and Charuta Chinchore, for having faith in me and my endeavors, without whose unconditional love and support I would not exist; my sister Apurva Chinchore who understood me like no one did and for standing like a pillar throughout my life.

COMPUTATIONAL STUDY OF SAVONIUS WIND TURBINES

ASMITA C. CHINCHORE

ABSTRACT

This project involves study of 2-Blade and 3-Blade Savonius vertical wind turbines positioned at different orientations. For a 2-Blade turbine the orientations considered were 0 degree, 45 degree, 90 degree and 135 degree in reference to the direction of the prevailing wind and for the 3-Blade turbine the orientations taken into account were 0 degree, 30 degree, 60 degree and 90 degree in reference to the direction of the prevailing wind. The basic aim of this thesis was to study how the two designs are different from each other and which design produces more power when applied with constant wind velocity of 10mps. Computational Fluid Dynamics (CFD) analyses were conducted for every case to find out the torque and power generated by the turbines for each orientation. To ensure the accuracy of the results, CFD techniques were applied using Gambit 2.2.30 and Fluent 6.2.16. All cases were run using “transition-SST” flow model and the faces were meshed using ‘Quadrilateral Pave’ meshing scheme. The turbine was also tested for varying wind velocities of 5mps, 20mps, and 30mps for a constant orientation of turbine. The results were later compared and graphs were created for easy comparison of power and torque generated by turbines at different velocities.

Maximum change in pressure occurs when 2-Blade turbine is perpendicular to direction of wind flow direction i.e. at 90 degree and when 3-Blade turbine is at 60 degree orientation. The 2-Blade Turbine generates higher value of torque (215.28 N) as compared to 3-Blade turbine, generating torque of value 110.92 N for any given constant wind velocity; 30mps in this case. This information can help the designer of the system to select the proper wind turbine considering the efficiency and stability along with other factors.

TABLE OF CONTENTS

ABSTRACT	v
LIST OF TABLES	viii
LIST OF FIGURES	ix
I INTRODUCTION	1
1.1 Identify the Problem/Need	3
II SCOPE OF PROBLEM	6
2.1 Design Concept	8
2.2 Introduction to Fluid Dynamics	9
2.3 Fluid Flow Analysis	11
III VALIDATION OF COMPUTATIONAL ANALYSIS (CFD) OF 3D DIMENSIONAL- CYLINDER IN FLUID DOMAIN	14
IV VALIDATION OF COMPUTATIONAL ANALYSIS (CFD) OF 3 DIMENSIONAL- TWO BLADE TURBINE	21

V	VALIDATION OF COMPUTATIONAL ANALYSIS (CFD) OF 3 DIMENSIONAL- THREE BLADE TURBINE	39
VI	RESULTS AND CONCLUSION	57
6.1	Conclusions	60
6.2	Future Scope	62
	REFERENCES	63
	APPENDICES	
A1	GLOSSARY	67
A2	NOMENCLATURE/ABBREVIATIONS	72
A3	POWER CALCULATION AND BETZ LIMIT	73

LIST OF TABLES

A2-1	Betz Power at varying Wind Velocities	74
A2-2	Generated Power at varying Wind Velocities	76

LIST OF FIGURES

1.1	Two Blade Vertical Axis Wind Turbine	2
1.2	Three Blade Vertical Axis Wind Turbine	3
1.1.1	U.S Energy Consumption by Energy Source, 2011	4
2.1.1	Two-Blade Savonius Wind Turbine	8
2.1.2	Two-Blade Savonius Wind Turbine	9
2.3.1	Domain Sizing	12
3.1	Mesh Element Types	15
3.2	Mesh of 3D-Cylinder in fluid domain	17
3.3	3D Cylinder-Velocity Magnitude, Plane 12	18
3.4	3D Cylinder- Static Pressure Distribution, Plane 12	19
3.5	3D Cylinder- Contour of Turbulent Kinetic Energy (k) (m^2/s^2), Plane 12	20
4.1	Different Angles of 2 Blade Turbine	22
4.2	Mesh of Two Blade Turbine at 0 Degree Orientation	23
4.3	2 Blade Turb. 0 Degree orientation- Vel. Magnitude, Plane 14 Contours	24

4.4	2 Blade Turb. 0 Degree orientation Static Pressure distribution, Plane 14	25
4.5	2 Blade Turb.0 Degree orientation - Vector Display Plane 14 [flow of wind over turbine]	26
4.6	Mesh of Two Blade turbine at 45 Degree Orientation	27
4.7	2 Blade Turb. 45 Degree Orientation -Vel. Magnitude, Plane 14 Contours	28
4.8	2 Blade Turb. 45 Degree Orientation-Static Pressure on Plane 14	29
4.9	Fig 2 Blade Turb. 45 Degree Orientation -Vector Display Plane 14 [Air Flow over turbine]	30
4.10	Mesh of Two Blade turbine at 90 Degree orientation	31
4.11	2 Blade Turb. 90 Degree Orientation -Vel. Magnitude, Plane 14 Contours	32
4.12	2 Blade Turb. 90 Degree orientation- Static Pressure distribution- Plane 14	33
4.13	2 Blade Turb. 90 Degree Orientation-Velocity Vector Plane 14 [Flow over the turbine]	34
4.14	Mesh of 2 Blade turbine at 135 Degree Orientation	35
4.15	2 Blade Turb. 135 Degree tile- Velocity Magnitude, Plane 14 Contours	36
4.16	2 Blade Turb. 135 Degree orientation- Static Pressure, Plane 14 Contours	37

4.17	2 Blade Turb.135 Degree Orientation– Velocity Vector Display, Plane 14 [Flow over turbine]	38
5.1	3 Blade Turbine in a Fluid domain	40
5.2	Mesh of Three Blade Turbine at 0 Degree Orientation	41
5.3	3 Blade Turb.–Initial Position-Velocity Magnitude, Plane 18 Contours	42
5.4	3 Blade Turb.-0 Degree Orientation- Static Pressure distribution, Plane 18	43
5.5	3 Blade Turb.0 Degree Orientation – Velocity Vector Display, Plane 18	44
5.6	Mesh of 3 Blade Turb. At 30 Degree Orientation	45
5.7	3 Blade Turb. 30 Degree Orientation– Velocity Magnitude, Plane 17	46
5.8	3 Blade Turb. 30 Degree orientation –Static Pressure, Plane 17 Contours	47
5.9	3Blade Turb. 30 Degree orientation- Velocity Vector Display. Plane 17	48
5.10	Mesh of 3 Blade Turb. at 60 Degree orientation	49
5.11	3 Blade Turb. 60 Degree orientation- Velocity Contours , Plane 17	50
5.12	3 Blade Turb. 60 Degree orientation- Static Pressure display, Plane 17	51

5.13	3 Blade Turb.-60 Degree Orientation-Velocity Vector Display Plane 17	52
5.14	Mesh of 3 Blade Turb. at 90 Degree orientation	53
5.15	3 Blade Turb. 90 Degree Orientation– Velocity Magnitude, Plane 17	54
5.16	3 Blade Turb. 90 Degree Orientation– Static Pressure, Plane 17	55
5.17	3 Blade Turb.- 90 Degree Orientation- Velocity Vector Display Plane 17	56
6.1	Wind Velocity (m/s) v/s Force on Turbine (N)	58
6.2	Wind Velocity (m/s) v/s Torque on Turbine (N.m)	59
6.3	Wind Velocity (m/s) v/s Power Generated (W)	60

CHAPTER I

INTRODUCTION

As known for generations wind turbines are devices that convert kinetic energy of wind into rotary mechanical energy. This mechanical energy can further be used to produce electricity, drive machinery, and charging devices etc. In today's world where conventional sources of energy are contributing to global warming, scientists are concentrating on extracting energy from non-conventional energy sources. Wind energy, solar energy, geothermal, municipal solid waste and biomass are among alternative energy sources. According to the scientific study wind energy has proven to be a viable energy alternative for many of the industrialized nations.

“Many studies have shown that wind energy is valued as one of the most dependable sources in today's world. In order to maintain this status, continued efforts to refine the design and production techniques are necessary. Wind and solar energy is likely to furnish one of the largest sources of manufacturing jobs worldwide. ”⁴

Though wind turbines are being widely used in many areas for power generation, its design remains a topic of debate. Wind turbines come in all different shapes and sizes. There are geared and direct drive wind turbines; horizontal axis and vertical axis wind turbines; upwind and downwind turbines; big and small ones. Some have one or two blades, and some have twelve blades or more! Some even have more than one rotor! Modern wind turbine engineers avoid building large machines with an even number of rotor blades. The most important reason is the stability of the turbine. Figure 1.1.1 and 1.1.2 show Savonius wind turbines with 2 blades and 3 blades respectively. In year 1922, Sigurd J. Savonius invented the Savonius rotor.²³ The rotor appears in the shape of 'S' in cross section, when viewed from top.



Fig1.1- 2 Blade Vertical Axis Wind Turbine



Fig1.2- 3 Blade Vertical Axis Wind Turbine

The total number of blades on a turbine may vary according to the application requirement. Though the number of blades can be increased, it does not necessarily contribute in increasing its efficiency. A turbine is said to have a good design if it produces maximum efficiency with minimum input cost. This thesis focuses on study of Vertical two-blade and three-blade Savonius wind turbines and comparison between their performances.

1.1 IDENTIFY PROBLEM/NEED

“As an increasingly accessible form of alternative energy, the wind power industry has grown enormously over the past decade. Results have shown that electricity generated using wind energy source is less costly, about four to six cents per kilowatt-hour, than the

other renewable energy sources ”.² In addition, wind turbines do not pollute the air like the burning of fossil fuel such as coal and natural gas .¹³ Most non-renewable sources create atmospheric pollution during their consumption. This includes smog, acid rain and global climate change. As a result, earth’s temperature has been gradually increasing over the past couple of decades.

The figure 1.2.1 shows a pie chart depicting the consumption of different energy sources in 2011. It illustrates that total energy consumed by renewable energy sources is 9% where as the percentage of energy consumption by non-renewable sources is 88.5%.

NOTE: Sum of components may not be equal to 100% due to individual rounding.

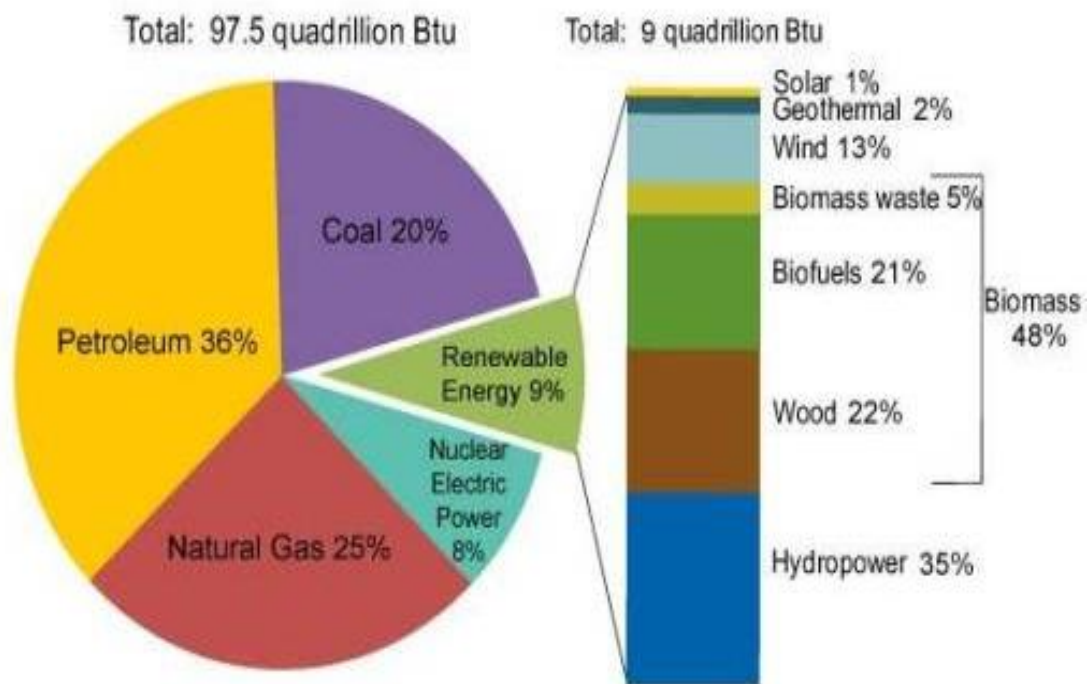


Fig 1.1.1 U.S Energy Consumption by Energy Source, 2011

Scientists have therefore focused their attention to make use of available resources. Wind is freely available in abundant and can be efficiently used with modern technology. The energy it produces creates no harmful pollutants or greenhouse gases. Wind energy is especially useful in remote areas that are not connected to electricity power grid.

CHAPTER II

SCOPE OF PROBLEM

This thesis studies effect of wind flow over vertical two-blade and three-blade Savonius Wind turbines. Each turbine is studied in a separate chapter. There is quite a difference in computational results of a certain design and practical implementation of the same. Thus the computational study of two blade turbine and three blade turbine is based on some important features and considerations which can be stated as follows:

- The Savonius wind turbine is a vertical wind turbine with the blade diameter of 24 inches and a total height of 60 inches. Considering the type of mesh which was quadrilateral ‘pave’ for all the cases, the height of the turbine was reduced to 15 inches. If the turbines were to be designed using the original height i.e. 60 inches, the meshing could have got affected since the mesh requires more than 4 CPUs (8 or 16 CPUs) to run the parallel processing of the turbine, which were not available at the time of study.
- The processor used to run the cases in Fluent was ‘Parallel Processor’ with 4 CPUs. Parallel processing in Fluent uses two or more number of CPUs simultaneously to

run a certain case. This reduces the computing time by dividing the job into small partitions and making the large scale job doable.

- There are two types of flow in nature, steady-state flow and transient flow. Steady state flow is preferred in cases which require low computational time and cost and are easy for post-processing of the results. Transient flow is used if the study involves aerodynamics, rotary machine, transient heat transfer and many more. This thesis uses ‘transient flow’ for all the cases as the flow of air is assumed to be unsteady over the period of time.
- The geometries and design models are drafted in Gambit considering that all the dimensions are in ‘inches’. But Fluent on the other hand does not read the dimensions as imported. The unit system of Fluent is set to ‘meters’ (SI) by default. Hence all the geometries need a scaling factor to maintain a balance in the geometry dimensions. A scaling factor of 0.0254 was used in all the cases which is the conversion factor from ‘inches’ to ‘meters’.
- The velocity at the input face in the boundary condition is assumed to be ‘10 m/s’ for all the cases.
- The solution method applies the scheme of ‘PISO’ and the solution gradient of ‘Green-Gauss Node Based’ in all the cases.
- The monitor reference value for convergence criteria was assumed to be ‘1e-06’.

Out of the four orientations for two-blade turbine, one case was put to test the effect of different velocities (5mps, 20mps and 30 mps) on the turbine. The results were later compared to each other which proved to be beneficial to analyze the turbine behavior if it was to face different velocities.

2.1 DESIGN CONCEPT

Savonius Wind Turbine is the simplest design which is a drag-type turbine. It consists of two or three curved surfaces placed such that they look like an “S” shape in cross-section. Since it is a vertical wind turbine it need not be placed in specific direction for wind flow. Because of the hollow-curvature shape, the blade faces more drag facing the wind (in the direction of the wind), and it faces less drag in the opposite direction of wind. The scoops are attached to a vertical axel which acts as a base as seen from figure 2.1.1.

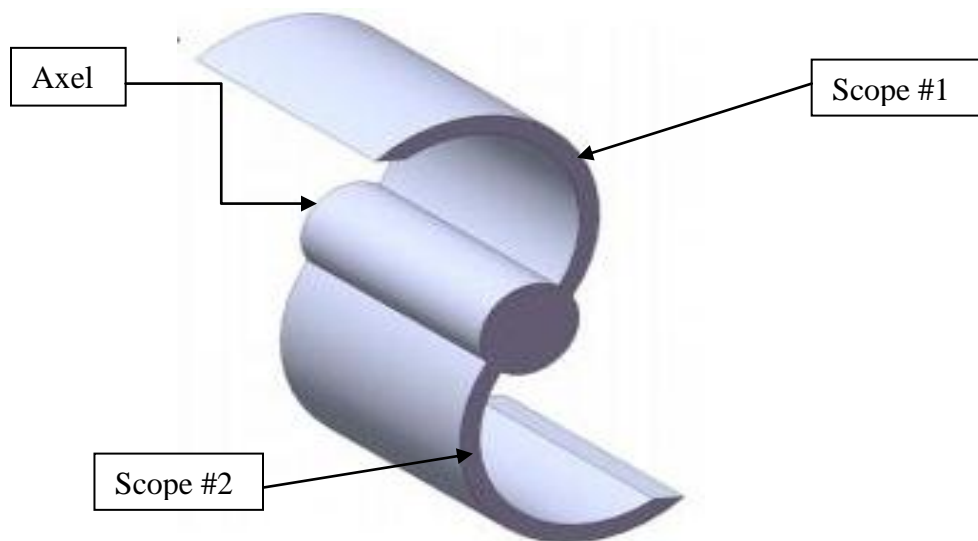


Fig 2.1.1- Two-Blade Savonius Wind Turbine

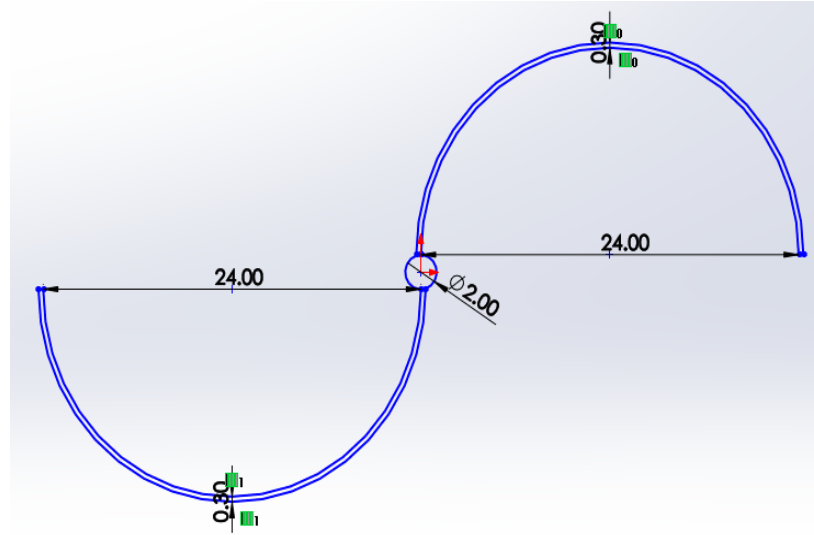


Fig 2.1.2- Two-Blade Savonius Wind Turbine

The figure 2.1.2 shows the design of a two-blade Savonius Wind turbine. The Pressure side (concave side) of the turbine has length of 24 inches with a thickness of 0.3 inches. The turbine was designed using a meshing software Gambit 2.4.6 which is explained in brief in the next chapter.

2.2 INTRODUCTION TO COMPUTATIONAL FLUID DYNAMICS

Computational Fluid Dynamics, a branch of Fluid Mechanics is defined as computer technology that provides a means to model and study the flow mechanics of nearly any type of physical problem. CFD has developed the way engineers used to solve complex fluid flow problems. For example, CFD software provides the mean to simulate the flow of gases and liquids, moving bodies, chemical reaction, heat and mass transfer, fluid-structure interaction, and acoustics through computer modeling.

The basic benefits of using CFD are that one gets enhanced understanding of a problem by creating a virtual model of the system. Behavior of the system can be visualized which provides understanding of the design, which is may be difficult otherwise. This is promising for the systems that are difficult to prototype or test through experimentation. By changing the input parameter to numerical model, predictions on the system can be obtained with in shorter time span. Anticipation can be stated as user's ability to predict how a design will perform as well as test several configurations until as optimal result is achieved. The results and history of various test configurations that is documented allows for more efficient future designs and testing (better, faster, and cheaper designs).

There are three subcomponents of CFD:

- a) *Pre-processing*: The main tasks involved in pre-processing are CAD or geometry creation, mesh generation and applying boundary conditions. For the purpose of this thesis a pre-processing and meshing software Gambit was used in the setup of all the models.
- b) *Solving (Simulation)*: The solving portion is the stage where the actual calculations are performed and data results are compiled. This step was performed using the Fluent's CFD code and solver. The mesh generated in Gambit was imported in Fluent for its further analysis.
- c) *Post-processing*: Fluent also provides the final step in an analysis which involves the post-processing stage. Fluent's post-processing software provides a number of tools that can be used to manipulate data and procedure color based CFD images and animations.

2.3 FLUID FLOW ANALYSIS

There are many fundamental means when approaching fluid flow problems which include infinitesimal system, experimental approach, control volume.

- Infinitesimal system is a very less known approach and is not used for complex problems. This technique includes recording details of a flow pattern, at every point, by analyzing as infinitesimal region of the flow.
- New FDEs (Fluid dynamic experiments) often need to confirm that they are accurately modeled according to real life phenomenon. Experimentation is used for that purpose. Though it involves initial setup costs, setup time and feasibility, experimentation provides exact results based on surrounding experimentation.
- Control volume method includes estimation of gross effects (mass flow, energy change, induced forces and moments) over a finite region.

The fluid flow analysis for flow around a 3D Cylinder, 3D Two-Blade Turbine and 3D Three-Blade Turbine will be performed using control volume method in CFD program Fluent. Creating specific geometry is the first step to begin with. NOTE: The geometry should be created to scale within the respected computer aided design software. The size of the geometry plays an important role to determine certain variables, which makes scaling important.

The length of the turbine is fixed in all the cases which provide a base for comparison. This fixed variable allows us to create a spatial domain for analyzing this problem. The size of the domain is determined following the formulae calculated years ago based on testing and experimentation.^{22,25} The domain size was initially kept small considering

time efficiency and computational demands, but the domain size was gradually increased to minimize the wall effects on solution results. Increasing the domain, results in increased computational time and more memory usage. The near perfect results are obtained making a compromise with CFD between:

1. Accuracy/Errors
2. Time Restraints
3. Hardware Availability

Figure 2.2 shows the domain for a cylinder, which demonstrates size of domain for external flow around cylinder.

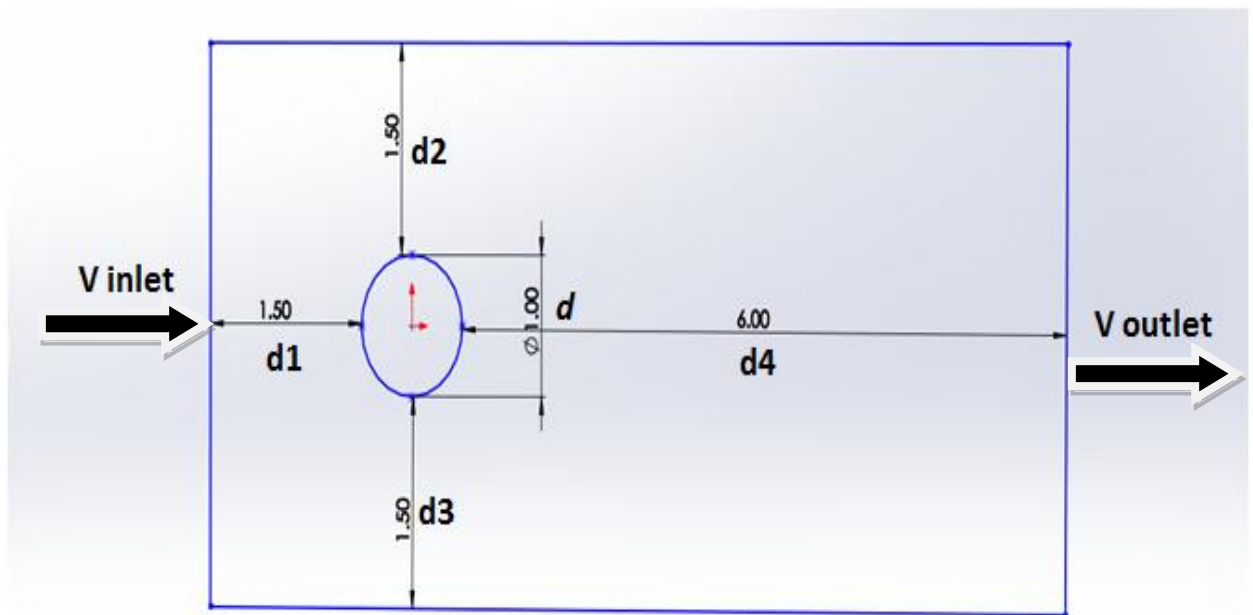


Fig 2.3.1- Domain Sizing

Figure 2.2 illustrates the distance between cylinder and the surrounding domain. Let us assume that the diameter of the cylinder ' d ' be 1 inch. Then the dimensions of the domain are as follows:

- Distance between Inlet face and cylinder $\mathbf{d1= 1.5*d}$
- Distance between Upper/Lower face and cylinder $\mathbf{d2=d3= 1.5*d}$
- Distance between Outer face and cylinder $\mathbf{d4= 6*d}$

To initiate the fluid flow analysis, parameters like cylinder size are added to the domain. Also it helps to determine the parameters that most accurately represent the problem. The next chapter (Chapter 3) presents the validation and results of a sample problem of cylinder. The cylinder is used for validation of the results generated by the computational method used in this work.

CHAPTER III

VALIDATION OF COMPUTATIONAL ANALYSIS (CFD) FOR 3D-CYLINDER IN FLUID DOMAIN

The domain, mesh, and B.C's were developed by implementing research of prior arts. A series of tests were performed to verify what had previously been produced.¹ The main aim of the tests was to reduce the setup time and computational time for user along with improving accuracy of the solution. Alternatives such as symmetry boundary conditions or short flow inlets can significantly save the user's time.

Driving parameters that were applied in these tests include:

1. Domain size and its ratio
2. Mesh type (map, submap, pave)
3. Mesh quality (transition between regions of importance)
4. Mesh size (element size, scaling ratio)
5. Boundary conditions

6. Continuum Types

Each parameter above can have an effect on the accuracy of the solution.

It is essential that user comprehends the solution process along with Fluent's code, before proceeding. The first step of grid (mesh) generation takes place in Gambit which is a pre-processing tool of Fluent. Gambit provides with GUI (graphic user interface) that helps to position the model in the required domain, also providing a three-dimensional environment. Once the model is complete, it can be applied with 2D/3D mesh elements as shown in Fig 3.1.

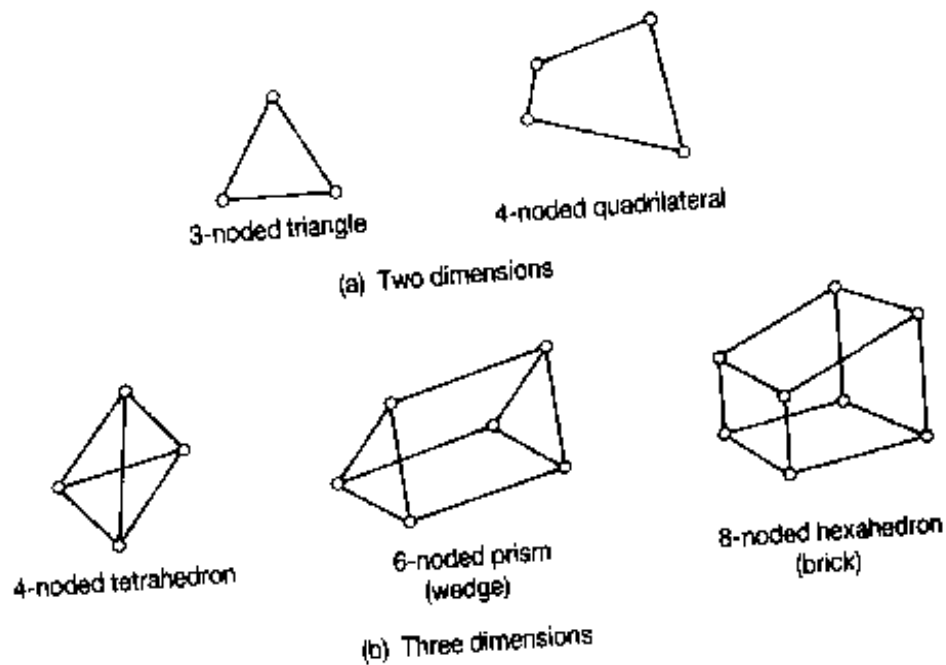


Fig 3.1- Mesh Element Type

The model can be exported in Fluent in a file format which is compatible with Fluent, upon finishing it with the required entities. Fluent uses internal data structures to assign an order to cells, faces, grid points in a mesh since it is an unstructured solver which

helps in relieving any restrictions or faults in the design of the model. This saves cost for the problems that are simple in nature and creates additional opportunity for those problems that were once deemed unsolvable due to the computational restrictions of the past.

The choice of mesh is dependent upon each individual model/specific application. In addition to the CFD discretization schemes, additional factors which can be computationally demanding are:

1. Setup time- varies according to new problems. This can be minimized by reducing errors and applying the correct mesh elements to the model.
2. Computational Expense (time, storage capacity, memory, number of CPU's etc) - A structured mesh generally provides result accuracy, less computational time and memory saving.
3. Numerical Diffusion- a form of truncation error is an error made by numerical algorithms that arises from taking a finite number of steps in computation. To reduce numerical diffusion, the flow should be aligned with mesh, refine the mesh, give enough time for computation and converging the solution.

Figure 3.2 is the case of cylinder introduced in a fluid domain. This example generated results which are reliable and the actual problem-cases can be compared with this case.

The mesh generation of the 3D Cylinder is displayed in the following figure 3.2:

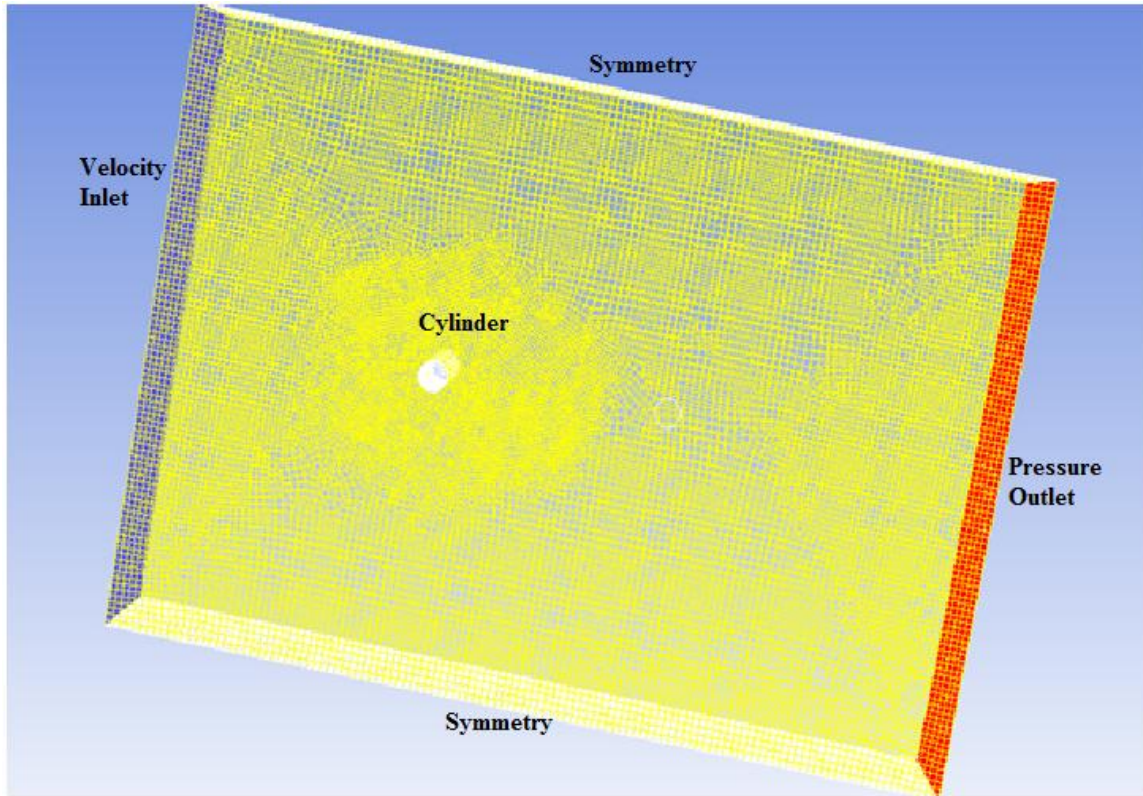


Fig 3.2- Mesh of 3D-Cylinder in fluid domain

All faces of the rectangular domain have different type of boundary conditions which can be stated as follows:

- Velocity Inlet-Fluid Inlet
- Pressure Outlet-Fluid outlet
- Symmetry- Side where cylinder is cut
- Symmetry- Side opposite of the cylinder
- Wall- Cylinder

The flow model that was used for this case was K-Epsilon model. The input velocity was uniformly distributed about the velocity inlet having a velocity of 10mps. The residual

criterion was set to a convergence criterion of 10^{-6} for each parameter. The faces are meshed using a quadrilateral ‘pave’ scheme. The edges that join the faces together are meshed using Successive Ratio meshing scheme in Gambit.

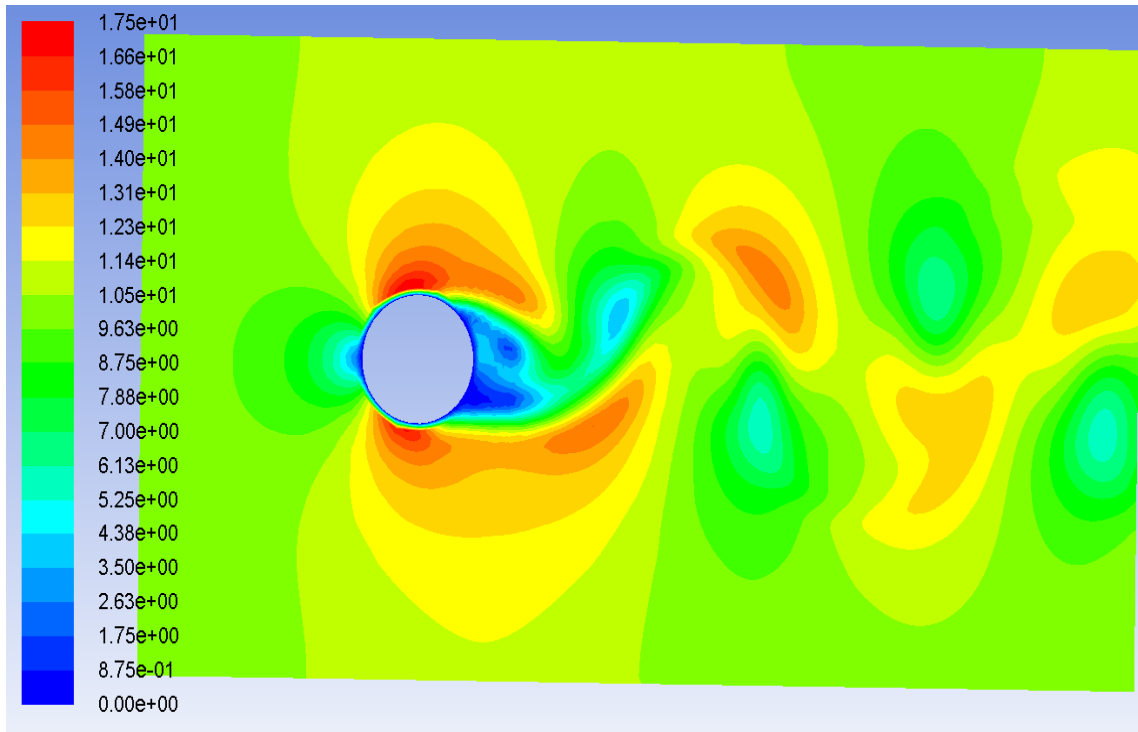


Fig 3.3- 3D Cylinder-Velocity Magnitude, Plane 12

The fig 3.3 illustrates the velocity distribution over plane 12°. The maximum velocity which is denoted by red color appears to have values of 17.599 mps ~ 18 mps. This maximum velocity occurs on the top side and bottom side of the cylinder.

°Plane 12- For the sake of analyzing and getting a clear vision of the flow pattern around the Cylinder, a plane of the domain was cut at a distance of 0.25 m from the back face of the domain. This cut plane represents plane12.

The area just to the left side of cylinder in upstream side is the area where the flow has direct impact reducing the flow velocity. The flow experiences strong flow oscillations and boundary layer separation in the wake region generated behind the body (on right side of cylinder, downstream side). A high velocity area is created along the pathway of the flow indicating the direction of the flow. The value of velocity decreases to almost zero in wake region.

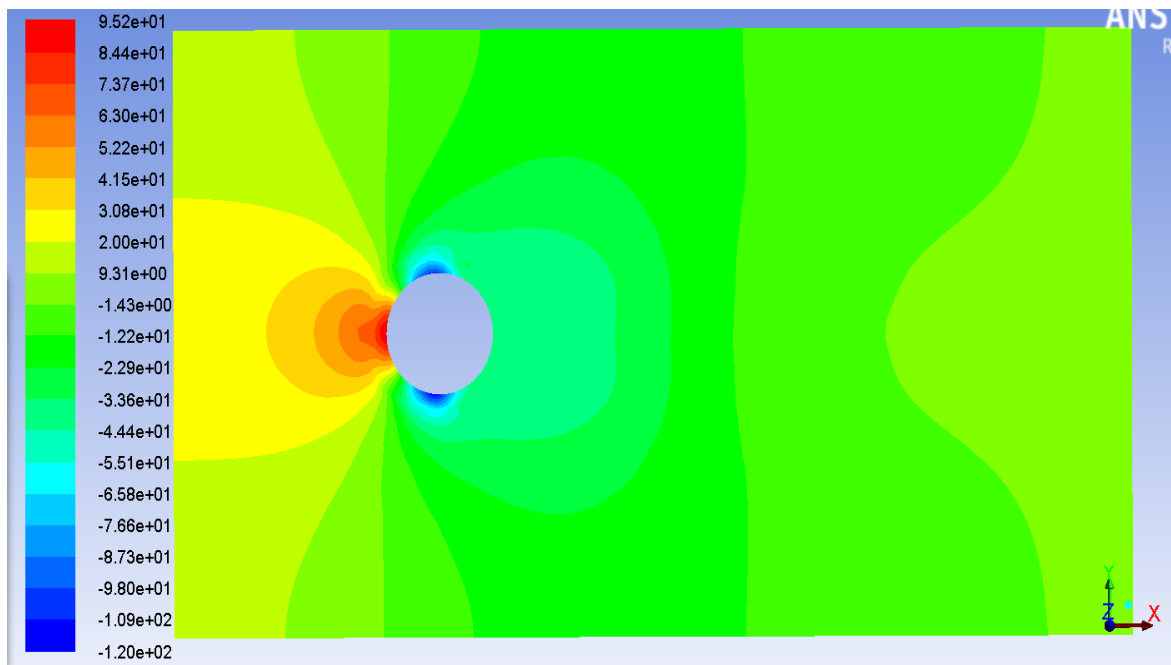


Fig 3.4- 3D Cylinder- Static Pressure Distribution, Plane 12

Figure 3.4 displays pressure distribution over plane 12. The fig shows that the negative pressure is distributed over the wake region whose value is roughly around -5.51×10^1 Pascal. Maximum negative pressure occurs on the top and bottom portion of the cylinder whose value is -1.20×10^2 Pascal. The maximum positive pressure occurs on the left side of the cylinder which faces direct flow. A red label indicates the maximum positive pressure whose value is 95.2 Pascal.

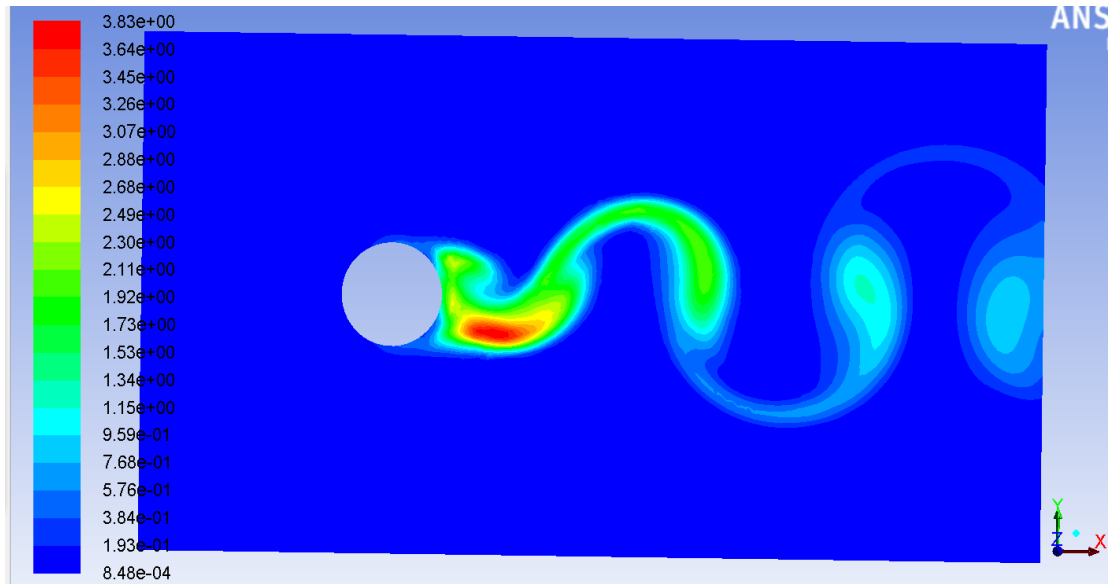


Fig 3.5- 3D Cylinder- Contour of Turbulent Kinetic Energy (k) (m^2/s^2), Plane 12'

The figure 3.5 represents contours of turbulent kinetic energy (k) over plane 12. The figure gives a clear idea about the direction of the flow of air after it passes the cylinder on the output side. It also shows that the maximum kinetic energy occurs in the wake region having a value of around $3.83m^2/s^2$.

The velocity magnitude, static pressure and turbulent kinetic energy all can be studied in extensive detail, which gives the user a very clear representation of the magnitude and direction of velocity vectors on the designated plane. This is extremely useful for more complex models such as k- ϵ model or transition-SST model in which the regions of reversed flow and vortices are clearly represented. The results acquired, for all the cases are obtained using CFD software. By comparing the results obtained of the cylinder with that from Kulkarni, A., & Moeykens¹⁹ and Masami Sato and Takaya Kobayashi²⁶, we can say that the results have been validated. The next step is to study the main problem of Savonius Wind Turbine in Chapter 4.

CHAPTER IV

VALIDATION OF COMPUTATIONAL ANALYSIS (CFD) OF 3D –

2 BLADE TURBINE

The domain, mesh and B.C's that were developed in the 3D cylinder model produced accurate results. However the system presented in this chapter involves a 2 Blade Savonius Turbine surrounded by the Fluid domain. The purpose of these studies was to find out the effects of application of wind on a Savonius turbine with two blades and analyze the velocity profile and pressure distribution on the blades.

To perform this analysis the 3D wind turbine configuration was considered in four different orientations, each case presenting the blades of a stationary Savonius turbine oriented at different angles to complete a 360 degree rotation. Several scenarios can be analyzed, but for the purpose of this document the four orientations that will be analyzed are: 0 Degree angle, 45 Degree angle, 90 Degree angle and 135 Degree angle for the orientation of the turbine in reference to the direction of the prevailing wind. If we add 45

Degrees to 135 Degree, the total is 180 Degree which is the same case as 0 Degree angle.
Hence only four cases are taken into account.

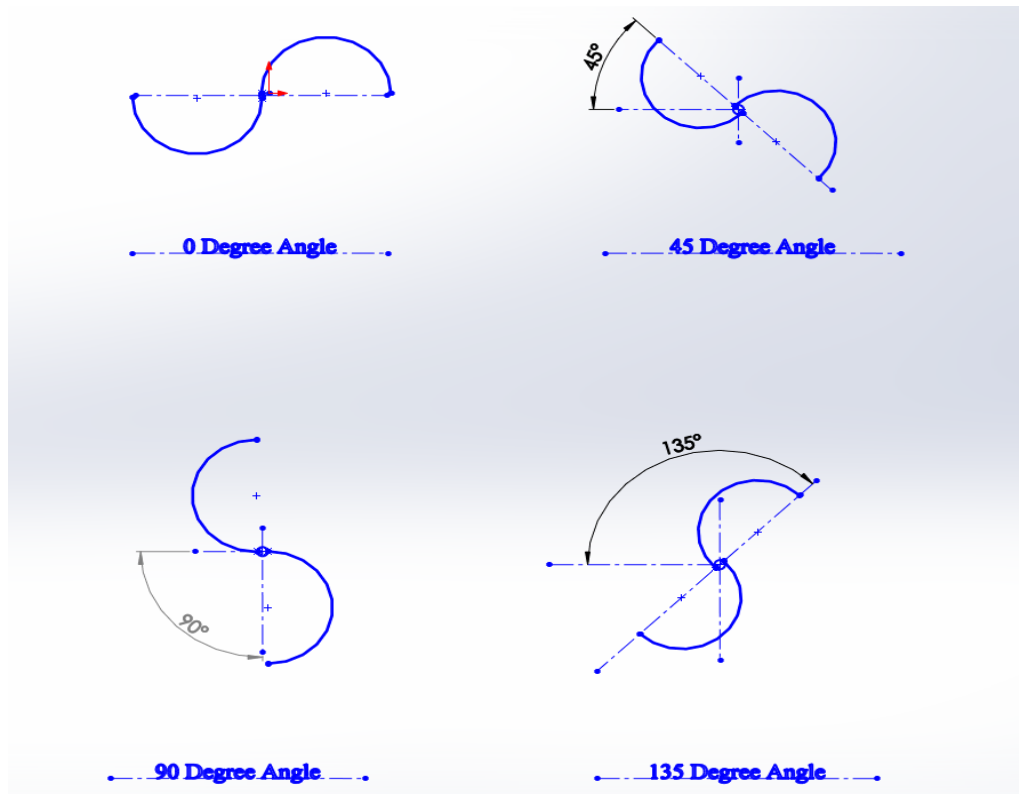


Fig 4.1– Different Angles of Two Blade Turbine

Figure 4.1 illustrates turbine rotated at four different angles. The research will specify that this type of problem requires a pressure outlet at the flow exit, velocity inlet or pressure inlet at the inlet and so on.

CASE I: 0 Degree Angle

In this case of 3D mesh all the faces are meshed using a quadrilateral ‘pave’ meshing scheme in Gambit. The edges that join the faces together are meshed using Successive Ratio meshing scheme in Gambit.

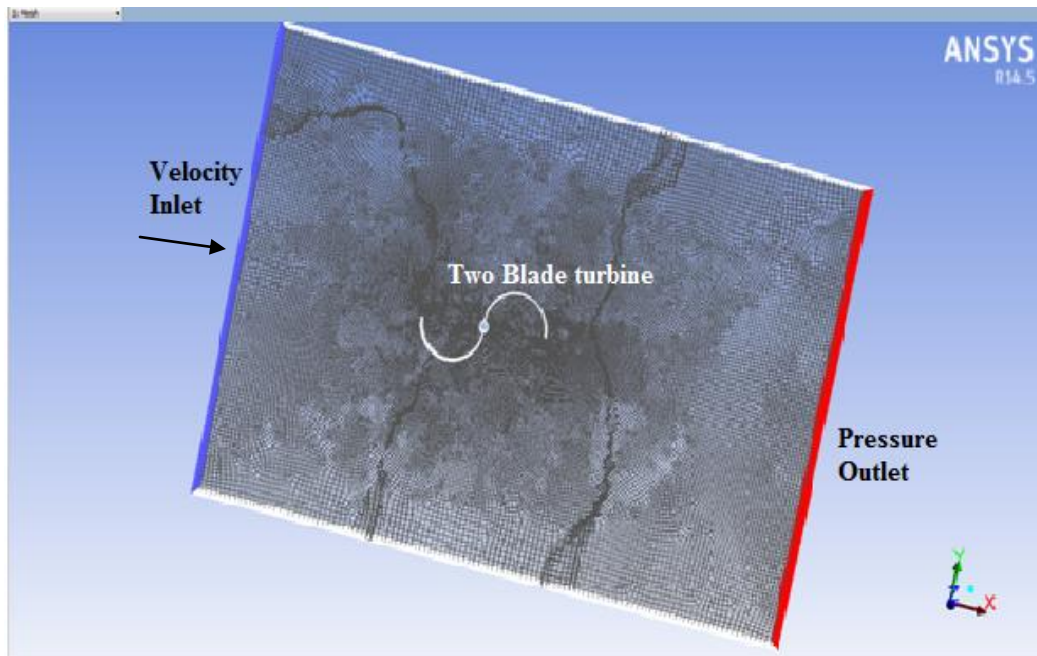


Fig 4.2 Mesh of Two Blade Turbine at 0 Degree Orientation

Fig 4.2 illustrate that meshing is dense in the proximity of turbine and is uniform throughout its width. Now that the mesh has been established, the boundary conditions can be applied as follows:

1. Velocity Inlet- Fluid inlet
2. Pressure Outlet-Fluid outlet
3. Symmetry-side where turbine is cut and opposite to it.

4. Wall-top and bottom of domain

5. Wall- turbine. NOTE: While applying boundary condition ‘Wall’ on turbine, it is

broken down into further detailed parts which are:

- a) Pressure Side- on concave surfaces on both the blades
- b) Suction Side- on convex surfaces on both the blades
- c) Tip Ends- tip width of both the blades
- d) Mid-Cylinder- on the cylinder where both the blades are attached

The flow model that was used for this case was transition-SST model. The input velocity was uniformly distributed across the inlet opening at 10mps. The residual criterion was set to a convergence criterion of 10^{-7} for each parameter.

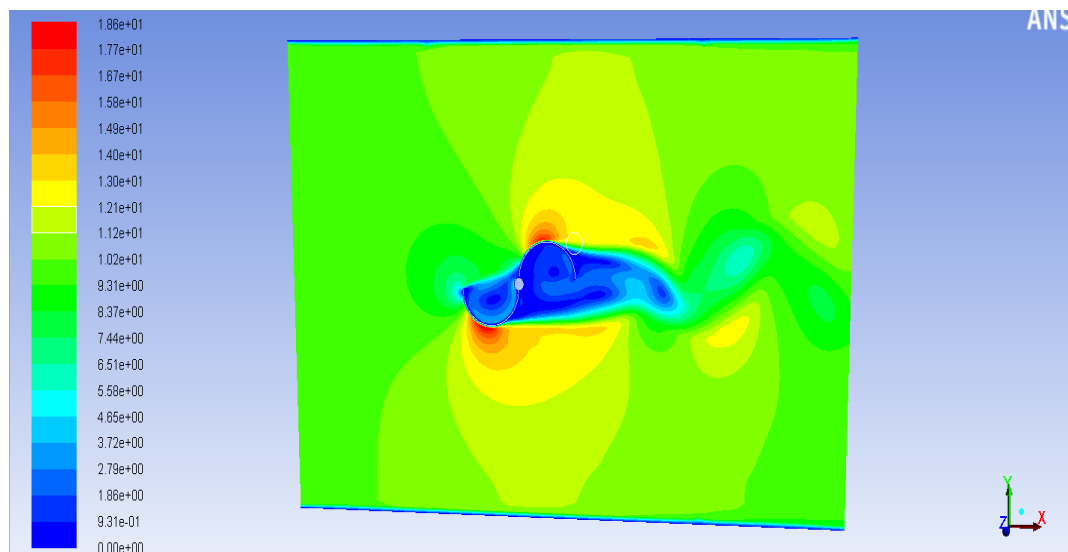


Fig 4.3- Two Blade Turb. 0 Degree orientation- Vel. Magnitude, Plane 14 Contours

°Plane 14- For the sake of analyzing and getting a clear vision of the flow pattern around the Cylinder, a plane of the domain was cut at a distance of 0.25 m from the back face of the domain. This cut plane represents plane14.

Fig 4.3 illustrates the velocity distribution over plane 14° of 3D turbine grid. The velocity magnitude is computed on all of the node points that exist within the default interior of the domain. It can be seen that the maximum velocity on the turbine is 18.61m/s. This further shows that the maximum velocity occurs at the suction sides (curved edges) of both the blades of turbine. A wake region is also produced in the region near turbine towards downstream where the velocity reduces to almost zero.

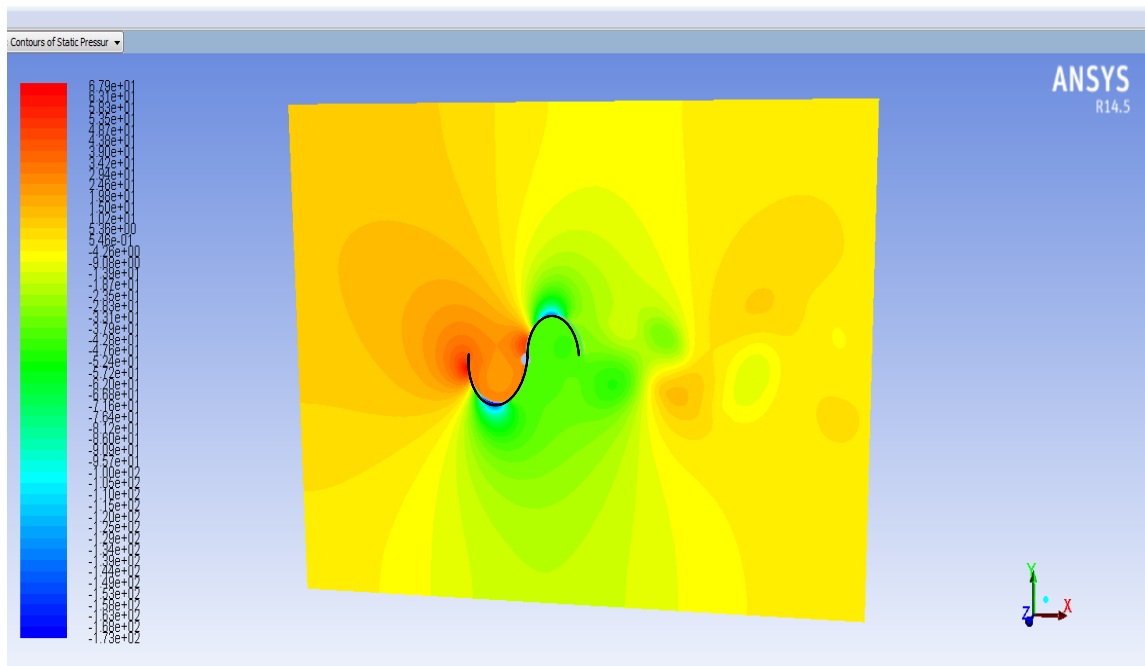


Fig 4.4- 2 Blade Turb. 0 Degree orientation Static Pressure distribution, Plane 14°

Figure 4.4 displays the Static pressure variation over the plane 14°. The results show that there is negative pressure developed in the area where wake region is produced. The maximum negative value occurs at the suction side (curved edges) of both blades which are -173.63 Pascal. This is the same areas of blades which faced maximum velocity on its surface. Further we can see that the static pressure in the upstream side near the tip of the

blade 1 is much more (67.89 Pascal) than the pressure in the wake region downstream side which is around -3.79 Pascal.

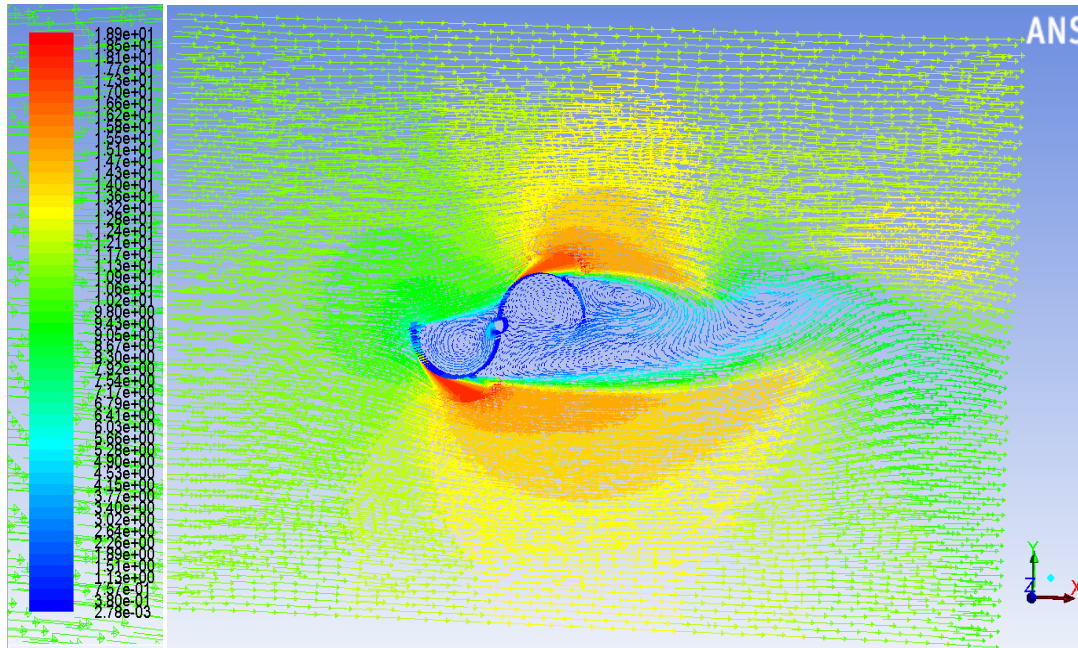


Fig 4.5- 2 Blade Turb.0 Degree orientation - Vector Display Plane 14 [flow of wind over turbine]

Figure 4.5 indicates the flow of air over the turbine displayed with arrow. It indicates that air enters from upstream side developing a reverse flow close to blades also creating pressure differences over the turbine. The velocity drops to almost $2.7e-3$ which is caused because of turbine positioning.

CASE II: 45 Degree Angle

This case includes a turbine whose blades are positioned at a 45 degree orientation with respect to the direction of the prevailing wind. The remaining conditions are same as CASE I. The meshing scheme of quadrilateral ‘pave’ is applied, along with boundary condition. The flow model that was used for this case was transition-SST model. The

following figure pictures the mesh of the turbine which is oriented at 45 Degree to study the effects of air flow at a certain angle.

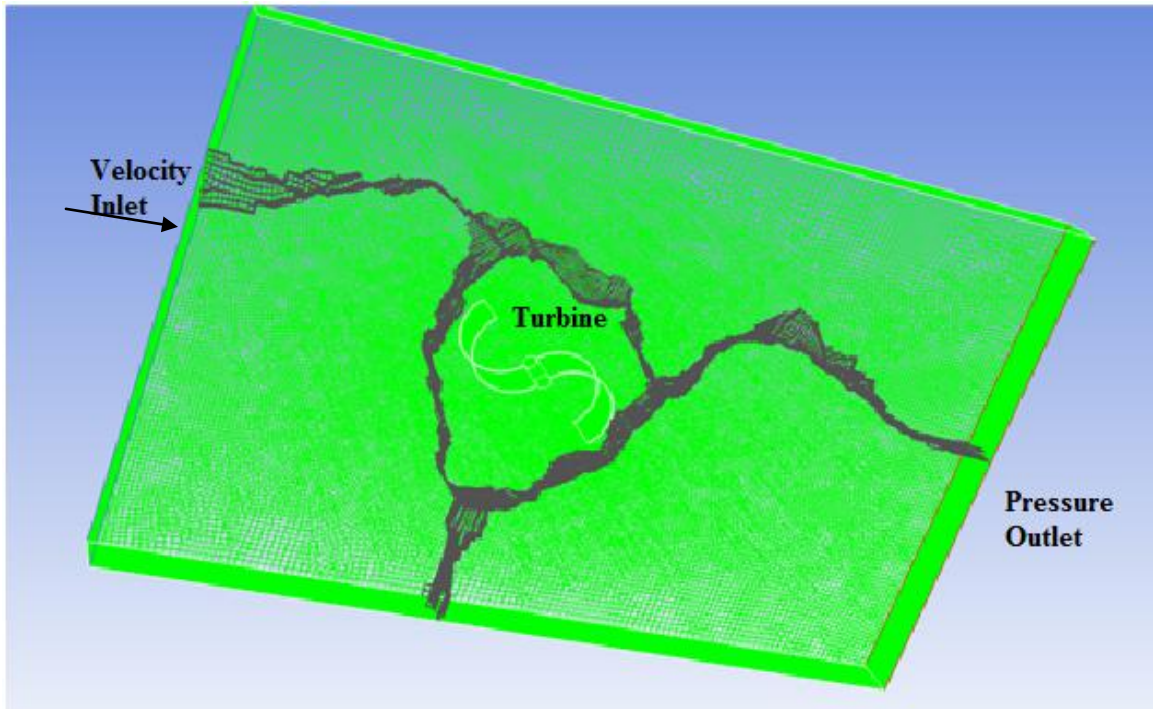


Fig 4.6- Mesh of Two Blade turbine at 45 Degree Orientation

The input velocity was uniformly distributed about the velocity inlet having a velocity of 10mps. The residual criterion was set to a convergence criterion of 10^{-7} for each parameter. The static pressure was used as surface monitor in Plane 14°.

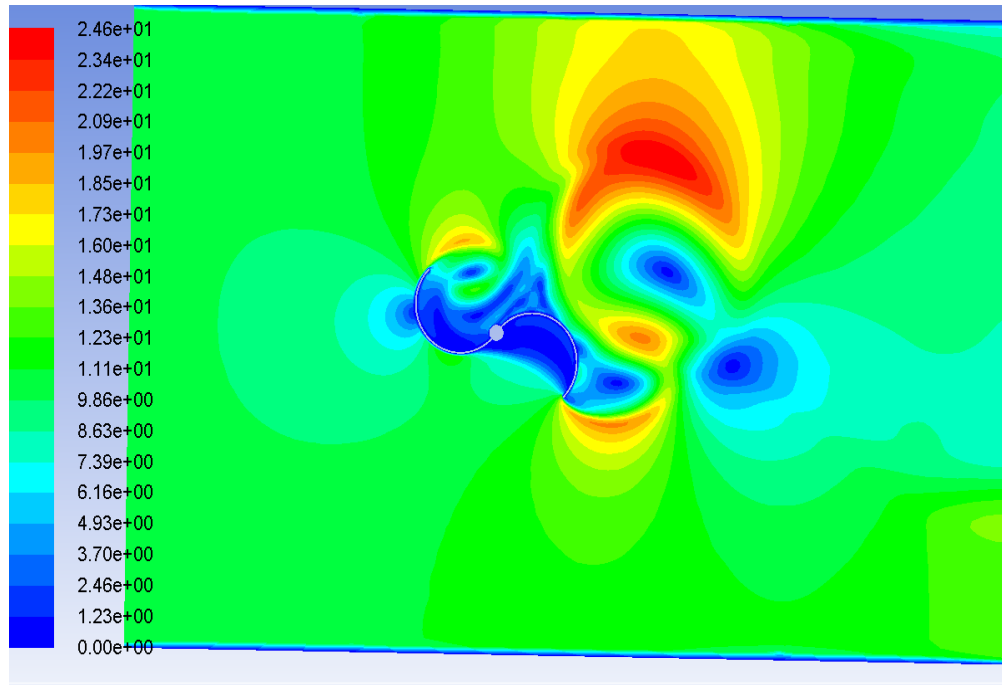


Fig 4.7- 2 Blade Trub. 45 Degree Orientation -Vel. Magnitude, Plane 14 Contours

The figure 4.7 shows that the 45 degree angle of turbine has shifted the high velocity area towards the upper side on downstream. The maximum velocity is 24.64mps. If we analyze the velocity at the tip of the blade 1 and 2, we can say that the velocity is roughly around 17.3mps, which is less than the maximum velocity. The air gets deflected upwards when it makes contact with blade1 and thus most of the wind gets diverted upwards, creating a high velocity region above the turbine.

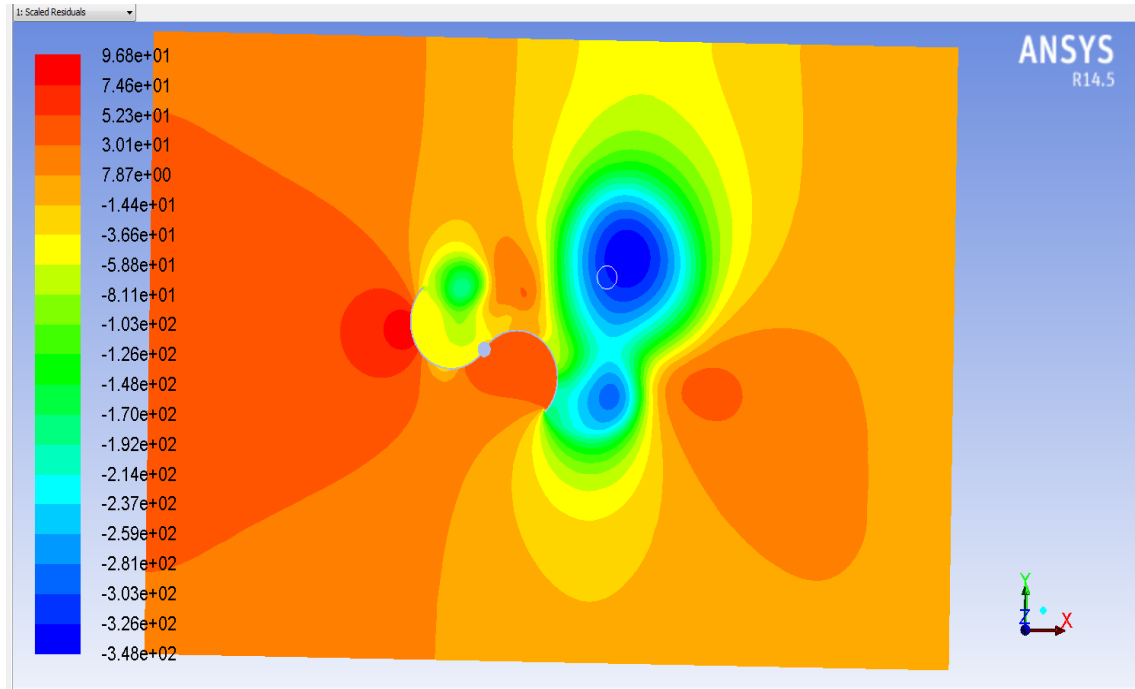


Fig 4.8- 2 Blade Turb. 45 Degree Orientation -Static Pressure on Plane 14°

Figure 4.8 displaying static pressure for 45 degree configuration shows that the maximum pressure is imposed on the suction side of blade 1 with a value of 96.79 Pascal. A negative pressure is imposed on the pressure side of blade1 with a value of around -3.66×10^1 . Furthermore, the suction side of blade 2 faces negative pressure and pressure side of blade 2 faces positive pressure. We can also see that the average pressure on downstream is less than the upstream side. The maximum negative pressure is generated in the wake region which is around -3.48×10^2 Pascal.

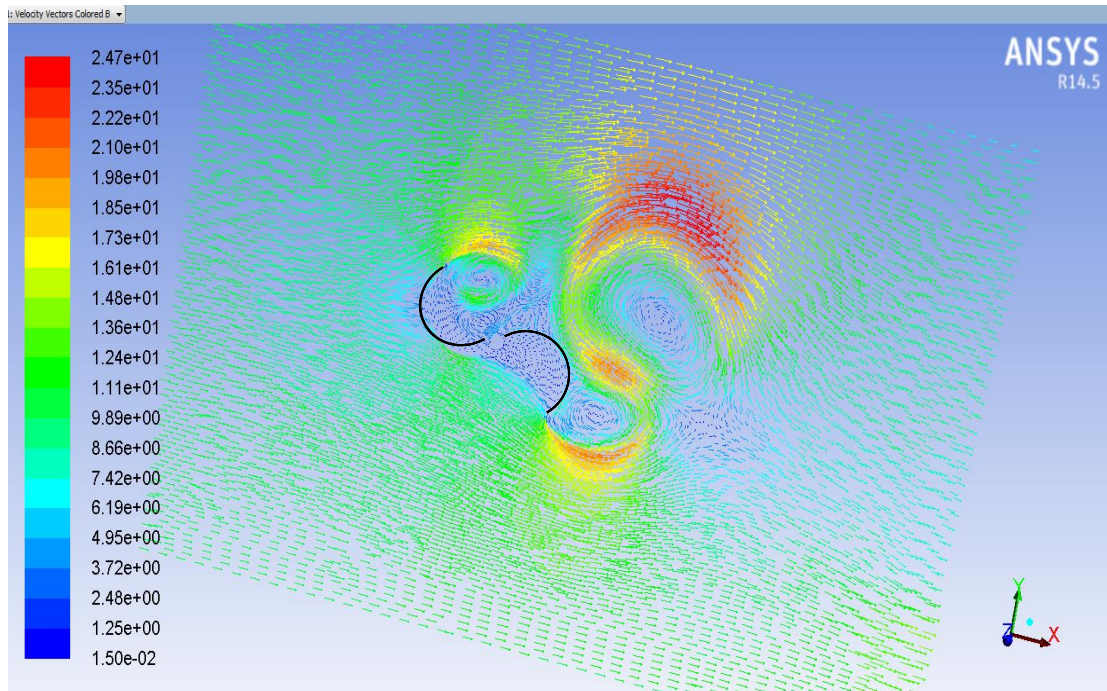


Fig 4.9- 2 Blade Turb. 45 Degree Orientation -Vector Display [Air Flow over turbine]

The figure 4.9 displays the velocity vectors and the direction in which the flow takes place. The reverse flow takes place in the pressure side of both the blades. The flow also diverts in a reverse direction in the wake region creating a negative pressure area.

CASE III: 90 Degree Angle

This case includes a turbine whose blades are positioned vertically i.e. at 90 degree configuration with respect to the direction of the prevailing wind. The remaining conditions are same as CASE I. The meshing scheme of quadrilateral ‘pave’ is applied throughout the model, along with the boundary conditions. The flow model that was used for this case was transition-SST model. The following figure pictures the mesh of the turbine which is vertical (90 Degree orientation) to study the effects of air flow at a certain angle.

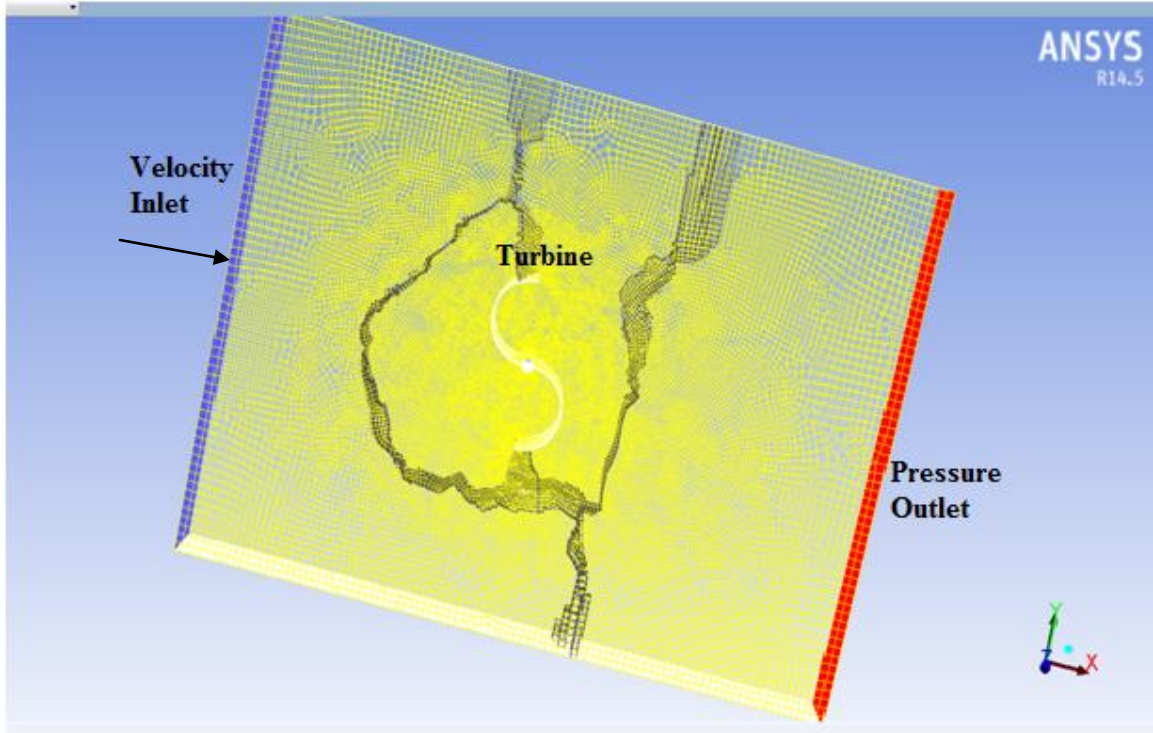


Fig 4.10- Mesh of Two Blade turbine at 90 Degree orientation

The input velocity was uniformly distributed about the velocity inlet having a velocity of 10mps. The residual criterion was set to a convergence criterion of 10^{-7} for each parameter. The data was monitored after every 50 time steps.

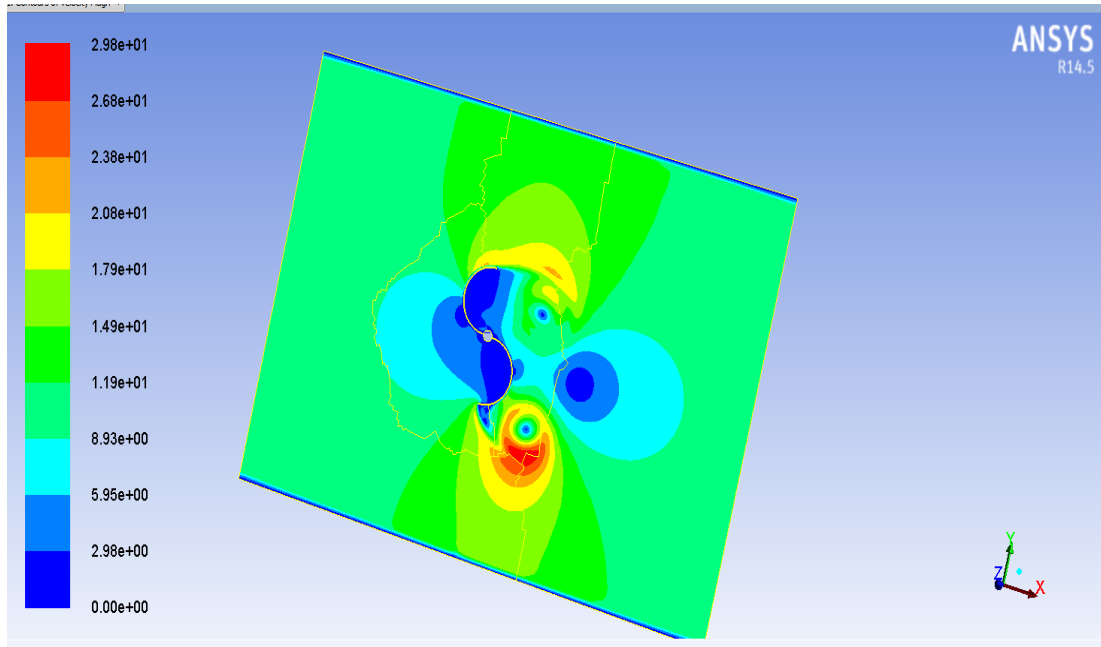


Fig 4.11- 2 Blade Turb. 90 Degree Orientation -Vel. Magnitude, Plane 14° contours

Figure 4.11 displays the velocity distribution over plane 14°. The value of maximum velocity is 29.75mps which occurs near the suction side of blade 2. A wake region is also generated in the downstream area of flow. The velocity tends to reduce to almost zero in the wake region. The tip of the blade 1 is imposed with velocity roughly around 20.8mps while the tip of blade 2 is imposed with velocity around 5.95mps. The area near the pressure side of blade 2 shows various velocities including minimum and maximum values at the same.

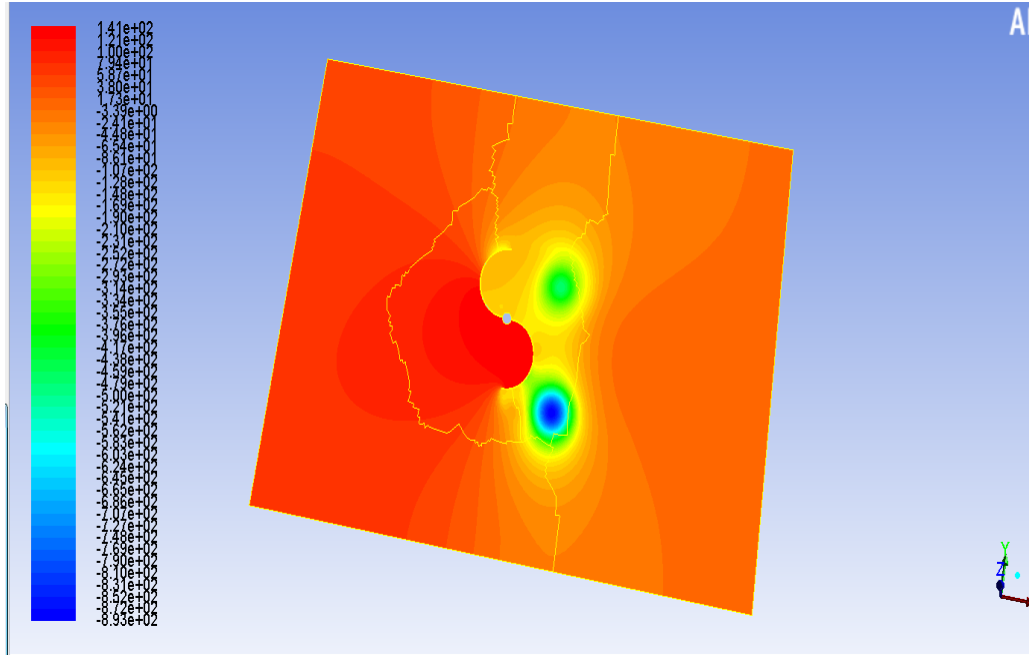


Fig 4.12- 2 Blade Turb. 90 Degree orientation- Static Pressure distribution- Plane 14

As we can see from figure 4.12 the suction side of blade 1 and the pressure side of blade 2 are enforced with maximum static pressure whose value is around 141.42 Pascal. In fact the upstream side has pressure higher than that on downstream side which is mostly negative pressure. Observe that the wake region was shifted from upper mid side (area near blade 1) in CASE II to lower mid side (area near blade 2) in this CASE III. The maximum negative pressure in the wake region is -892.95 Pascal which is maximum negative pressure considering all four cases. The pressure side of blade 1 is enforced with pressure value -4.48e+01 Pascal.

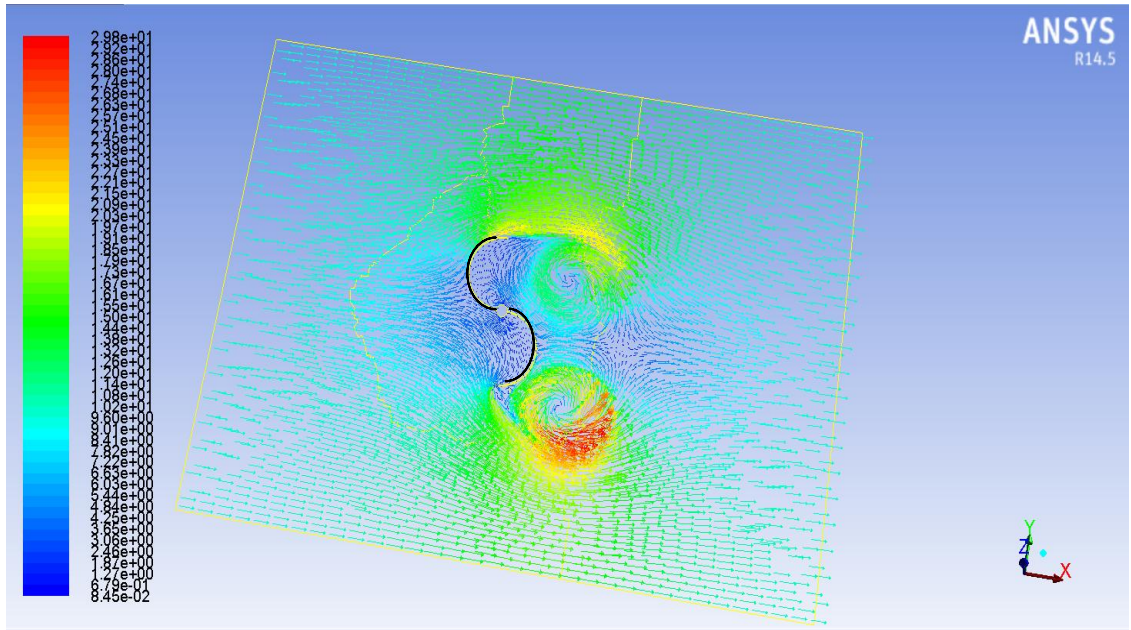


Fig 4.13– 2 Blade Turb. 90 Degree Orientation-Velocity Vector [Flow over the turbine]

The figure 4.13 displays the flow of air over the turbine on plane 14 in velocity vector form. The velocity vectors are rendered with extensive detail, which gives the user a very clear representation of magnitude and direction on the designated plane. This is extremely important for complex models of reverse flow and vortices are clearly represented.

CASE IV: 135 Degree Angle

The boundary conditions and flow model are the same that were applied to CASE I. The only change in the parameter was the position of the turbine. The Savonius wind turbine is orientated by 135 degrees with respect to the direction of the prevailing wind. The grid maintains a zone/mesh structure that is similar to that of the previous 3D turbine structured mesh. Rest all the conditions are kept as in previous cases. The meshing scheme of quadrilateral ‘pave’ was applied along with the flow model of transition-SST.

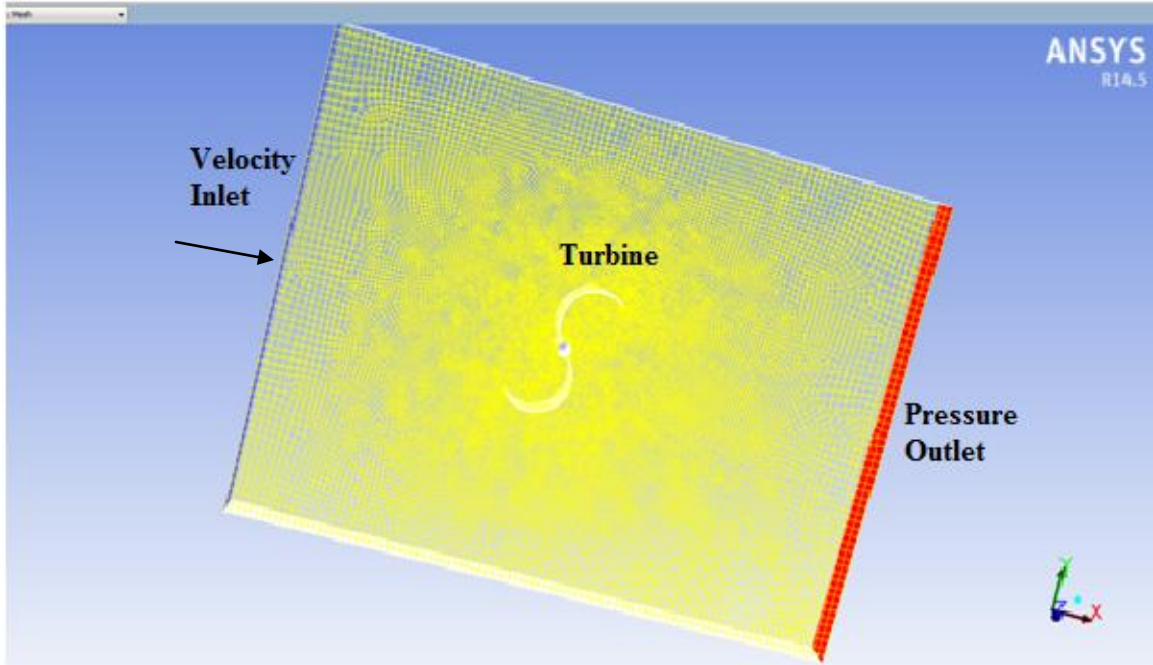


Fig 4.14-Mesh of 2 Blade turbine at 135 Degree Orientation

Figure 4.14 pictures the mesh of the turbine which is oriented at 135 degree to study the effects of air flow at a certain angle. The input velocity was uniformly distributed about the velocity inlet having a velocity of 10mps. The residual criterion was set to a convergence criterion of 10^{-7} for each parameter. The data was monitored after every 50 time steps.

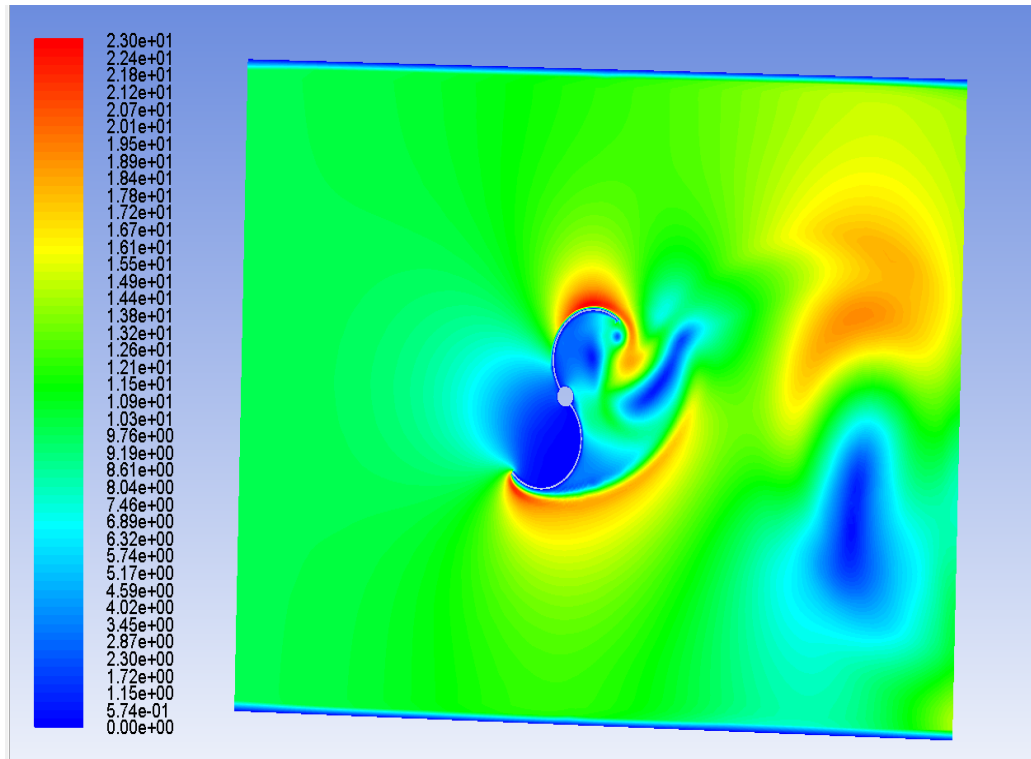


Fig 4.15– 2 Blade Turb. 135 Degree tile- Velocity Magnitude, Plane 14 Contours

The figure 4.15 shows the velocity distribution over plane 14° of two blade turbine. The maximum velocity, which is displayed by the legend in red, is shown to have a value around 22.96mps. This velocity appears in close proximity of suction side of blade 1 and also at the tip of the blade 2. The flow causes more impact in blade 1 as most of its blade is exposed to incoming velocity from upstream. A high velocity area is created in the downstream side close to the output face. This is the indication of wake region as the velocity drops to almost zero in the area, just below the high velocity area. The velocity drops close to zero in the area near suction side of blade 2 and pressure side of blade 1.

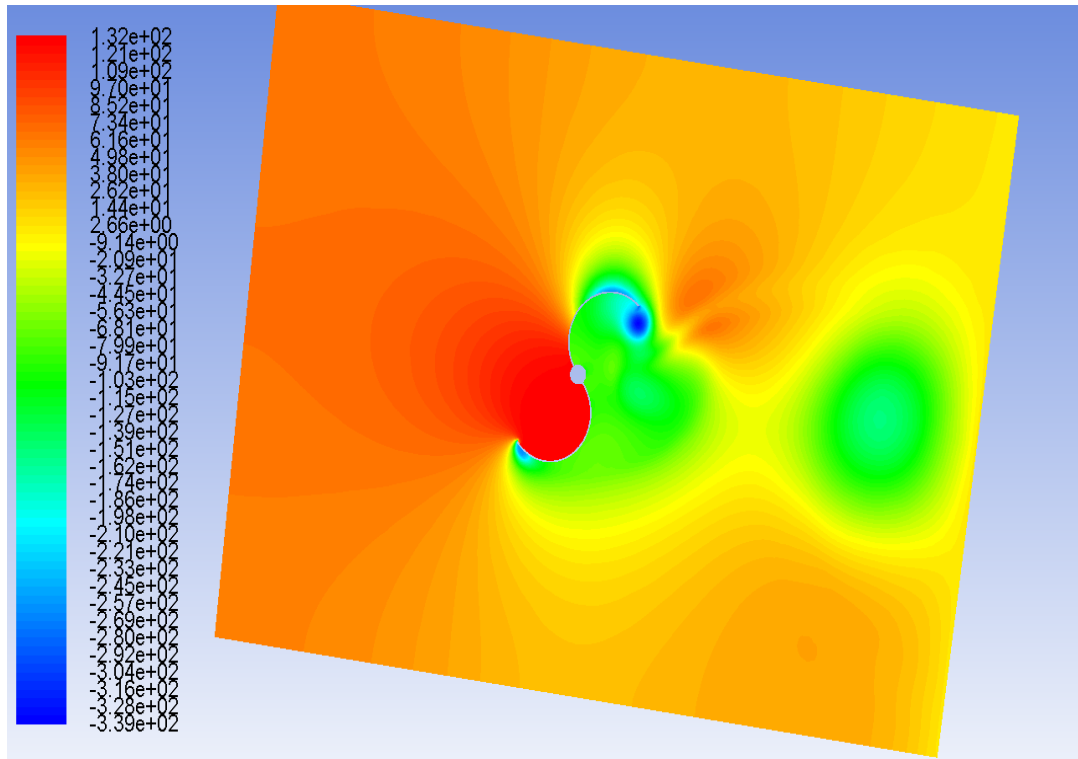


Fig 4.16– 2 Blade Turb. 135 Degree orientation- Static Pressure, Plane 14 Contours

Figure 4.16 represents distribution of static pressure over plane 14. The maximum pressure, which is displayed by legend in red, is shown to have a value of 132.38 Pascal. The maximum pressure is faced by the pressure side of blade 2. The rest of the turbine faces negative pressure. The highest negative pressure is imposed on the tips of both the blades whose value is -339.35 Pascal. The pressure side of blade 1 and suction side of blade 2 face a negative value of around -79.9 Pascal. The negative pressure continues on the downstream side including the wake region where the pressure attains high negative values. The case also shows the result that pressure on the upstream side (input) is more than that on the downstream side (output).

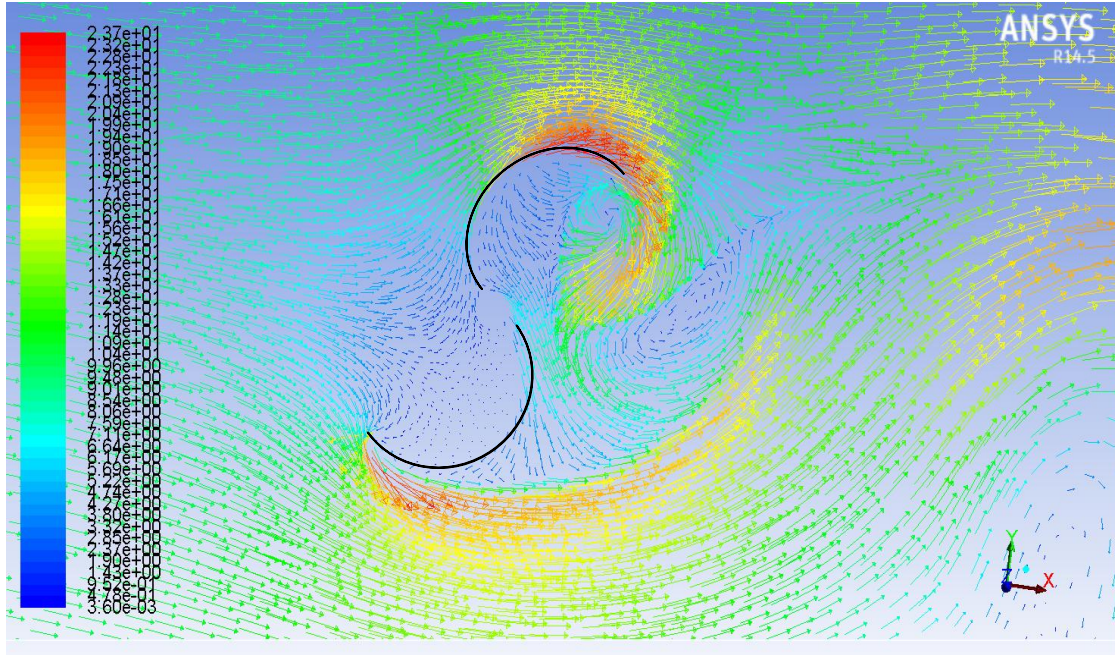


Fig 4.17- 2 Blade Turb. 135 Degree Orientation–Velocity Vector Display, Plane 14 [Flow over turbine]

Figure 4.17 displays the flow of air over the turbine on plane 14 in velocity vector form. The velocity vectors are rendered with extensive detail, which gives the user a very clear representation of magnitude and direction on the designated plane.

CHAPTER V

VALIDATION OF COMPUTATIONAL ANALYSIS (CFD) OF

3D - 3 BLADE TURBINE

The domain, mesh and B.C's that were developed in the 3D cylinder model and also in the 2 Blade Turbine with blade orientation at different angles, gave a picture of the fluid flow and its effects over a period of time. However this chapter involves a 3 Blade Savonius Turbine surrounded by the Fluid domain. Again the purpose of these studies was to find out the effects of application of wind on a Savonius turbine with three blades and analyze the velocity profile and pressure distribution, forces and moments etc.

To carry out this analysis a model of wind turbine was broken down into four cases, each case presenting the blades of a Savonius turbine oriented at different angles to complete a 360 degree rotation. Several scenarios can be analyzed, but for the purpose of this document the four cases that will be analyzed are: 0 Degree angle, 30 Degree angle, 60

Degree angle and 90 Degree angle for the orientation of the turbine in reference to the direction of the prevailing wind.

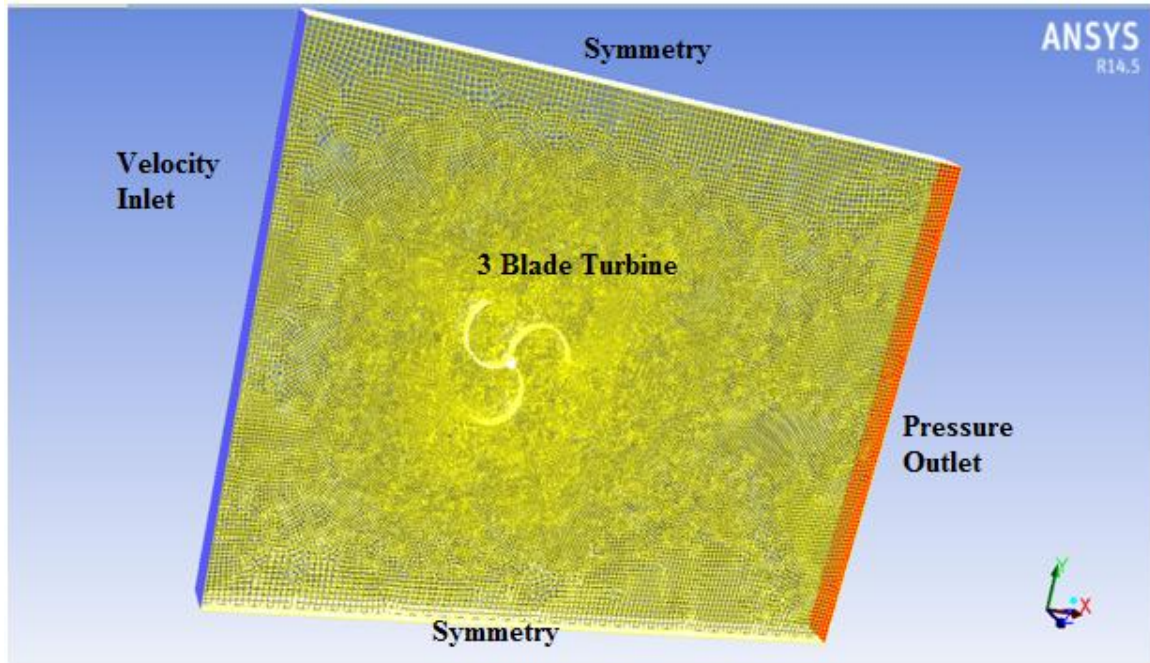


Fig 5.1- 3 Blade Turbine in a Fluid domain

As seen from the figure 5.1, all sides of the domain have different boundary types on different faces. The research will specify that this type of problem requires a pressure outlet at the flow exit, velocity inlet or pressure inlet at the inlet face and so on.

CASE I:3 Blade Turbine- 0 Degree Angle

The case applies a 3D mesh where all the faces are meshed using a quadrilateral ‘pave’ meshing scheme. The edges that join the faces together are meshed using ‘Successive Ratio’ meshing scheme in Gambit.

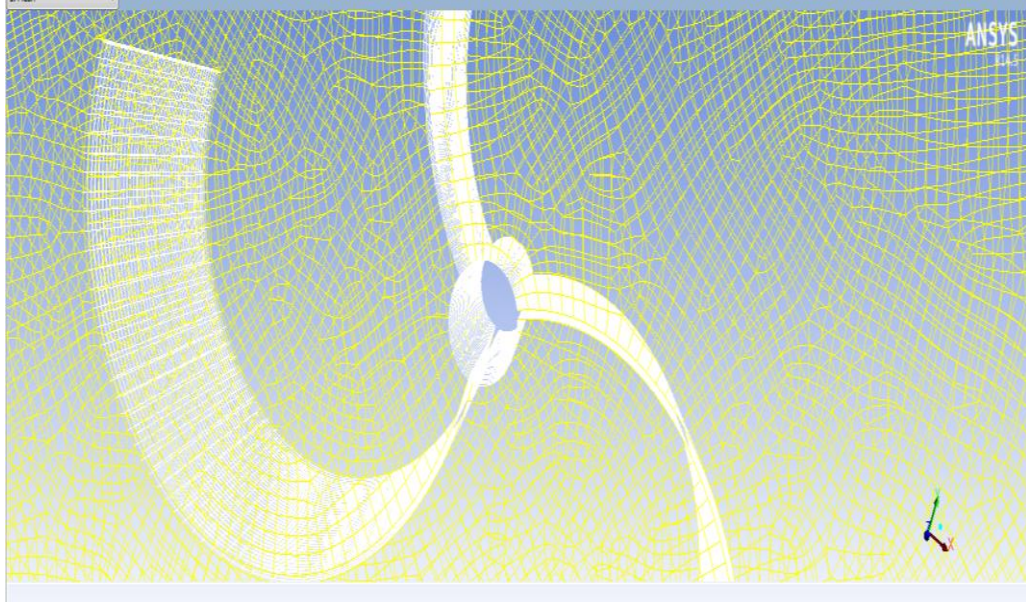


Fig 5.2-Mesh of Three Blade Turbine at 0 Degree Orientation

Fig 5.2 illustrate that meshing is dense in the proximity of turbine and is uniform throughout its width. Now that the mesh has been generated, the boundary conditions can be applied as follows:

1. Velocity Inlet- Fluid inlet
2. Pressure Outlet-Fluid outlet
3. Symmetry-side where turbine is cut and opposite to it.
4. Symmetry-top and bottom of domain
5. Wall- turbine. NOTE: While applying boundary condition ‘Wall’ on turbine, it is broken down into further detailed parts which are:
 - Pressure Side- on concave surfaces of all the three blades
 - Suction Side- on convex surfaces of all the three blades
 - Tip Ends- tip width of the three blades
 - Mid-Cylinder- on the cylinder where the blades are attached

The flow model that was used for this case was transition-SST model. The input velocity was uniformly distributed across the inlet opening at 10mps. The residual criterion was set to a convergence criterion of 10^{-7} for each parameter.

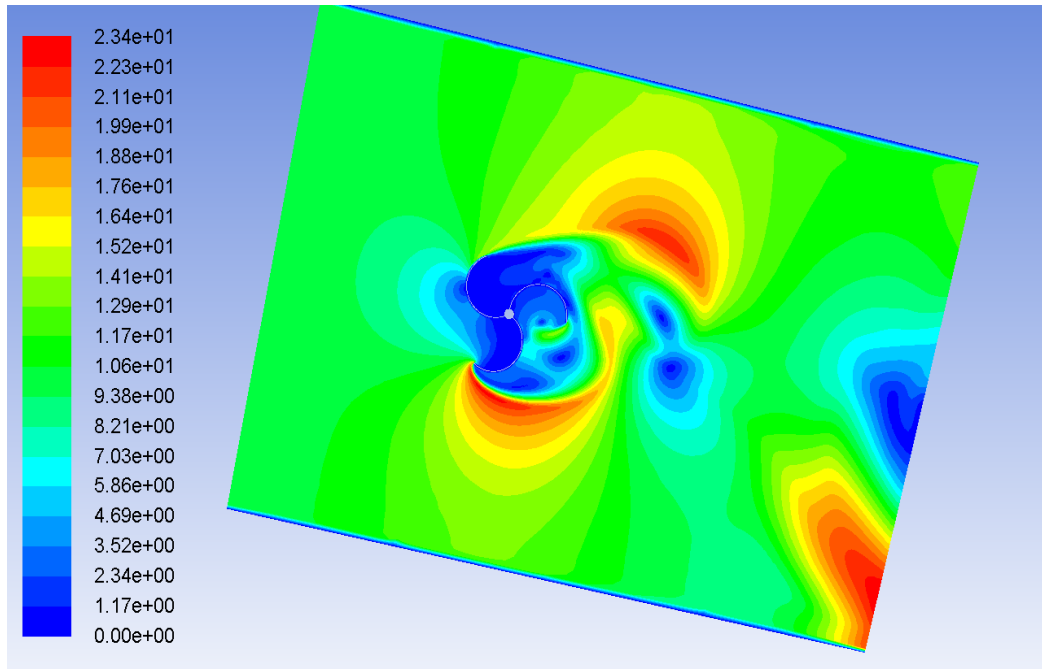


Fig 5.3– 3 Blade Turb.–Initial Position-Velocity Magnitude, Plane 18' Contours

Fig 5.3 illustrates the velocity distribution over plane 18' of 3D turbine grid. The velocity magnitude is computed on all of the node points that exist within the default interior of the domain. It can be seen that the maximum velocity on the turbine is 23.45m/s which is developed above the turbine. Further we can see that the maximum velocity occurs at the tip of blade-3 which continues to form a high velocity region on the bottom side of

blade- 3.

°Plane 18- For the sake of analyzing and getting a clear vision of the flow pattern around the Cylinder, a plane of the domain was cut at a distance of 0.25 m from the back face of the domain. This cut plane represents plane18.

The wind gets deflected by blade-1 towards positive Y-axis (upwards) creating a high velocity area above the turbine. A wake region is also produced on the right side of the turbine i.e. towards downstream where the velocity falls to almost zero.

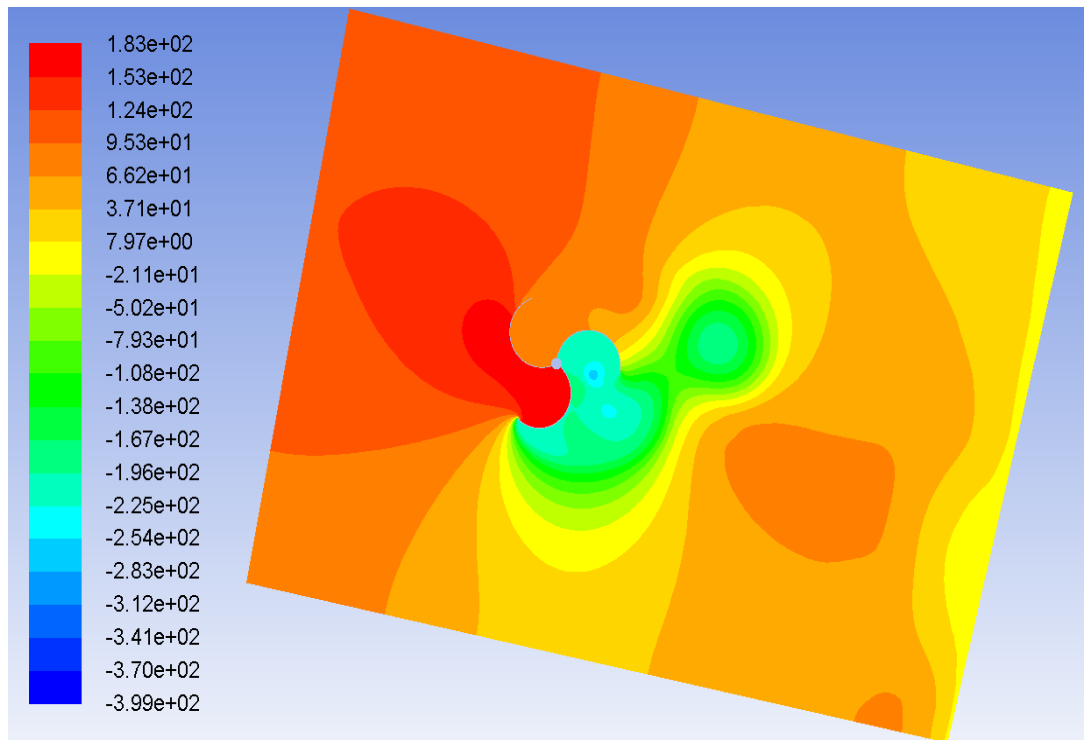


Fig 5.4- 3 Blade Turb.-0 Degree Orientation- Static Pressure distribution, Plane 18'

The fig 5.4 displays variation of static pressure over plane 18'. The results show that there is negative pressure developed on the downstream side (output) of turbine and positive pressure on the upstream side (input) of turbine. The maximum negative pressure is developed just to the right side of turbine with a value of -254×10^2 Pascal. This is the area which faces maximum turbulence and has created a wake region on the downstream. The maximum positive pressure is developed in the area between blade-1 and blade-2 whose value is 182.58 Pascal, which is much greater than the pressure developed on the downstream side.

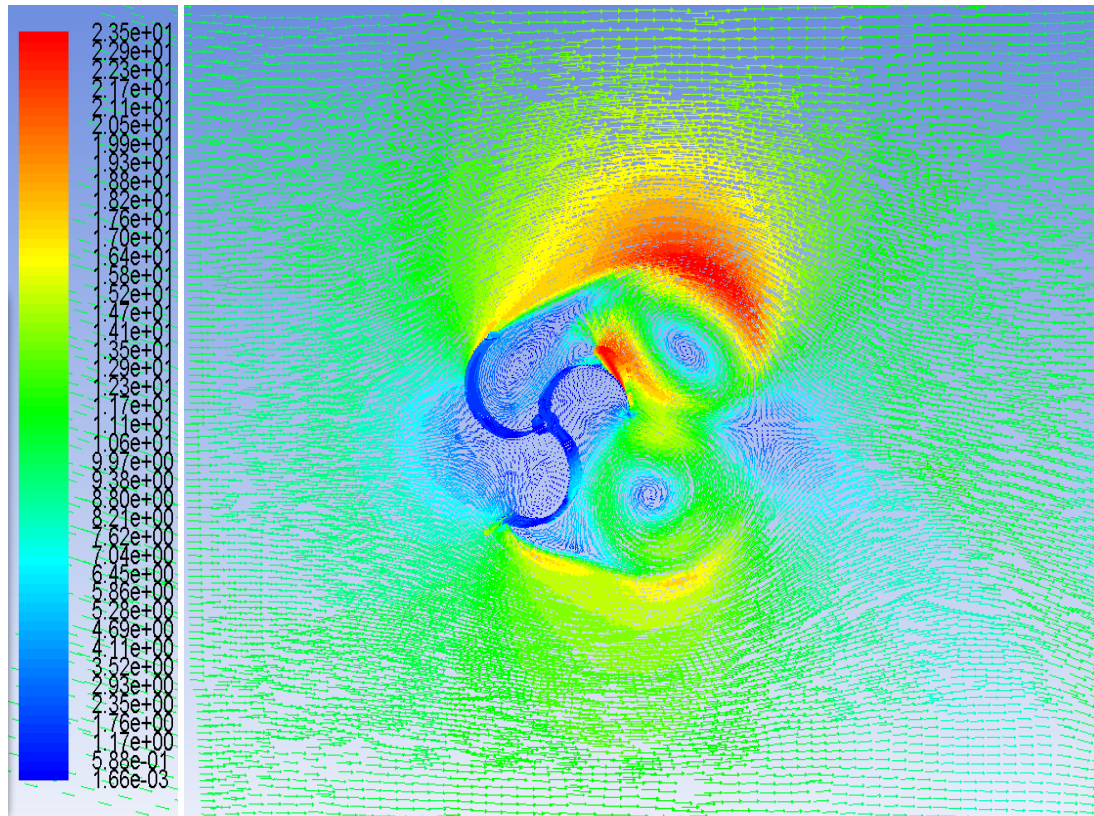


Fig 5.5- 3 Blade Turb.0 Degree Orientation – Velocity Vector Display, Plane 18'

The figure 5.5 displays the flow of air over the turbine on plane 18' in velocity vector form. The velocity vectors are rendered with extensive detail, which gives the user a very clear representation of magnitude and direction on the designated plane. The figure indicates that a reverse flow is developed in between the area of blade-2 and blade-3. The reverse flow is also developed on the downstream side of turbine.

CASE II:3 Blade Turbine- 30 Degree Angle

This case includes a turbine whose blades are positioned at a 30 degree orientation with respect to the direction of the prevailing wind. The rest conditions are same as CASE I. The meshing scheme of quadrilateral 'pave' is applied, along with boundary condition. The flow model that was used for this case was transition-SST model. The following

figure pictures the mesh of the turbine whose blades are oriented at 30 Degree to study the effects of air flow at a certain angle.

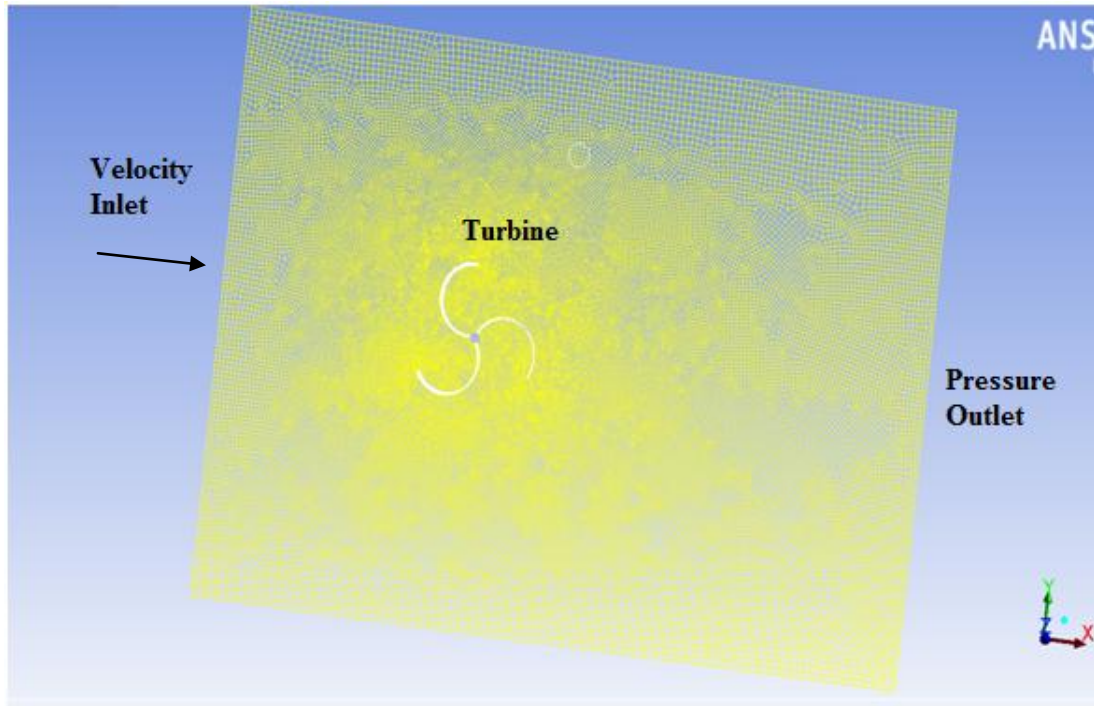


Fig 5.6- Mesh of 3 Blade Turb. At 30 Degree Orientation

An input velocity of 10mps was uniformly distributed over the inlet face. The residual criterion was set to a convergence criterion of 10^{-7} for each parameter. The data was monitored after every 50 time steps.

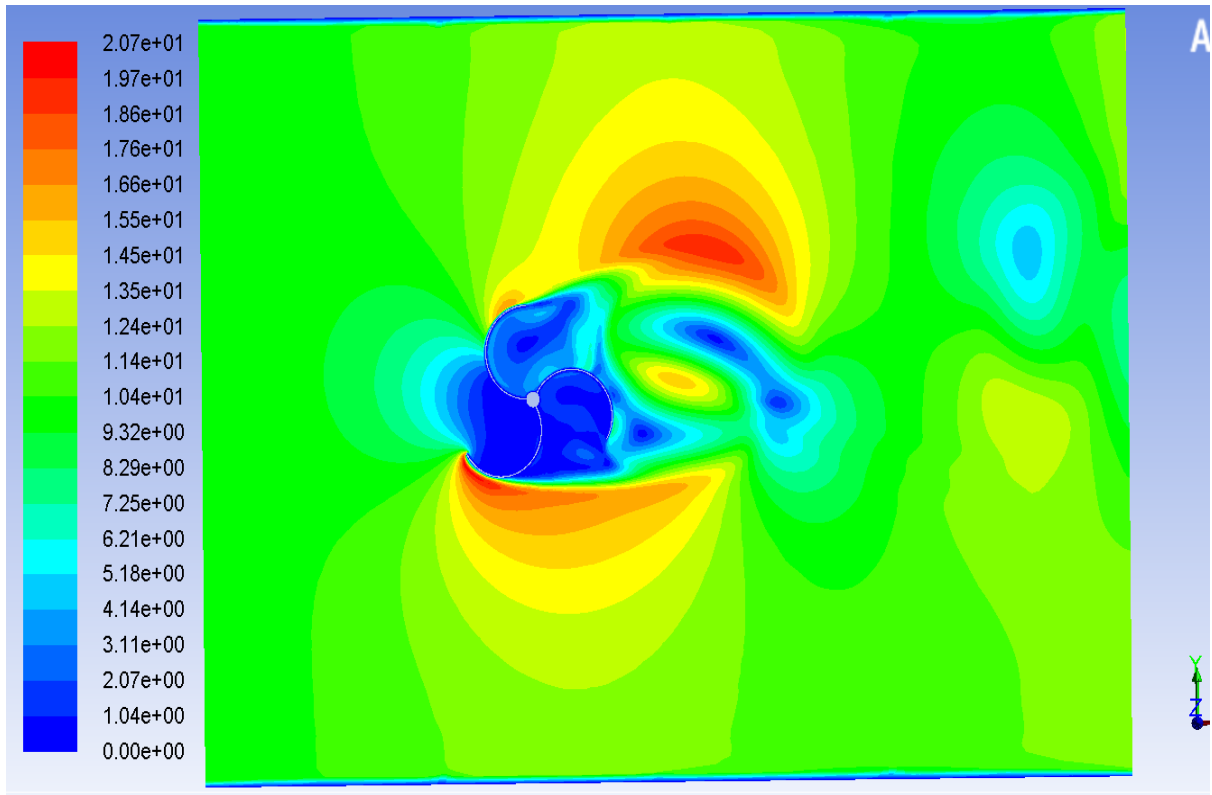


Fig 5.7– 3 Blade Turb. 30 Degree Orientation– Velocity Magnitude, Plane 17

The fig 5.7 shows that at 30 degree orientation of blades, a high velocity area was created near the tips of blade-1 and blade-3. If we analyze the velocity at the tip of the blade 1 and 3, we can say that the velocity is roughly around 15.5 mps, which is less than the maximum velocity. The area near the blades has velocity ranging from zero to a maximum value of 5.18 mps. This reduction in velocity can also be seen on the downstream side (output face) of the turbine. The air gets deflected upwards when it comes in contact with blade-1 and thus most of the wind gets diverted upwards, creating a high velocity region above the turbine.

*Plane 17- For the sake of analyzing and getting a clear vision of the flow pattern around the Cylinder, a plane of the domain was cut at a distance of 0.25 m from the back face of the domain. This cut plane represents plane17.

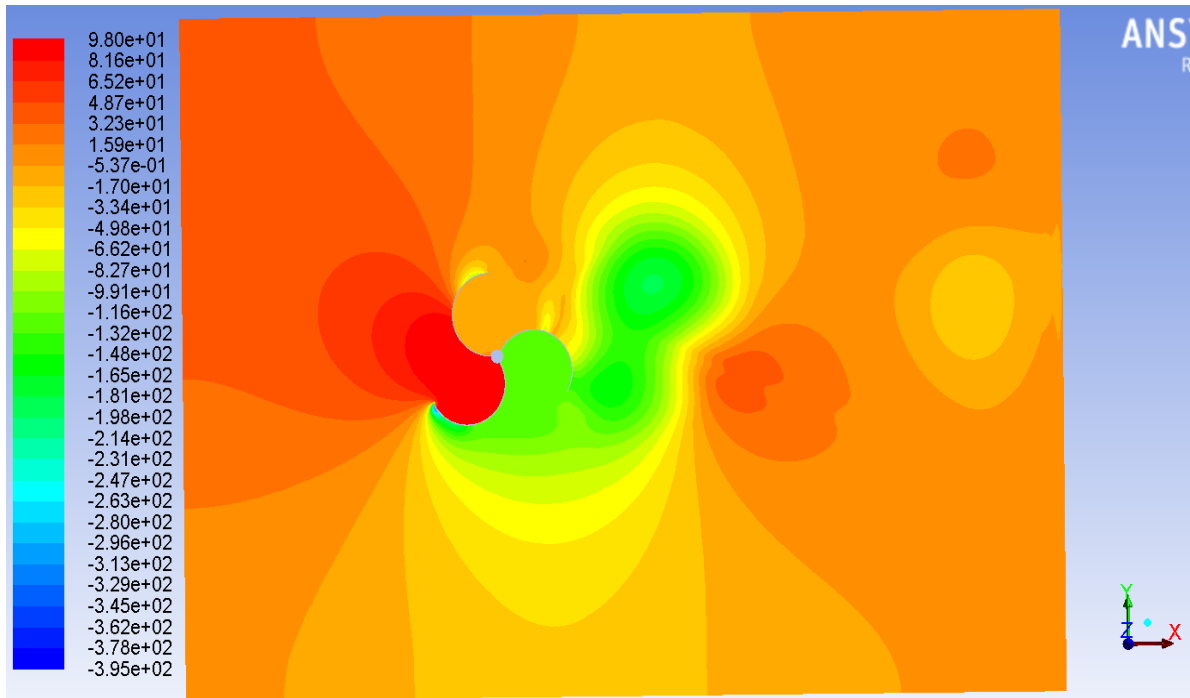


Fig 5.8-3 Blade Turb. 30 Degree orientation –Static Pressure, Plane 17 Contours

As seen from the figure 5.8 the maximum static pressure of value 98 Pascal is imposed in the area between blade-1 and blade-3. The suction side of blade-3 faces negative pressure roughly of value -2.47×10^{-2} Pascal. Thus we can say that blade-3 is facing high stresses due to high positive pressure on pressure side of blade-3 and high negative pressure on suction side of blade-3. The static pressure also drops to negative value in the wake region created just to the right side of the turbine. Observe that the value of negative pressure developed in area between blade-2 and blade-3 is more in CASE I as compared to this CASE II (30 Degree orientation).

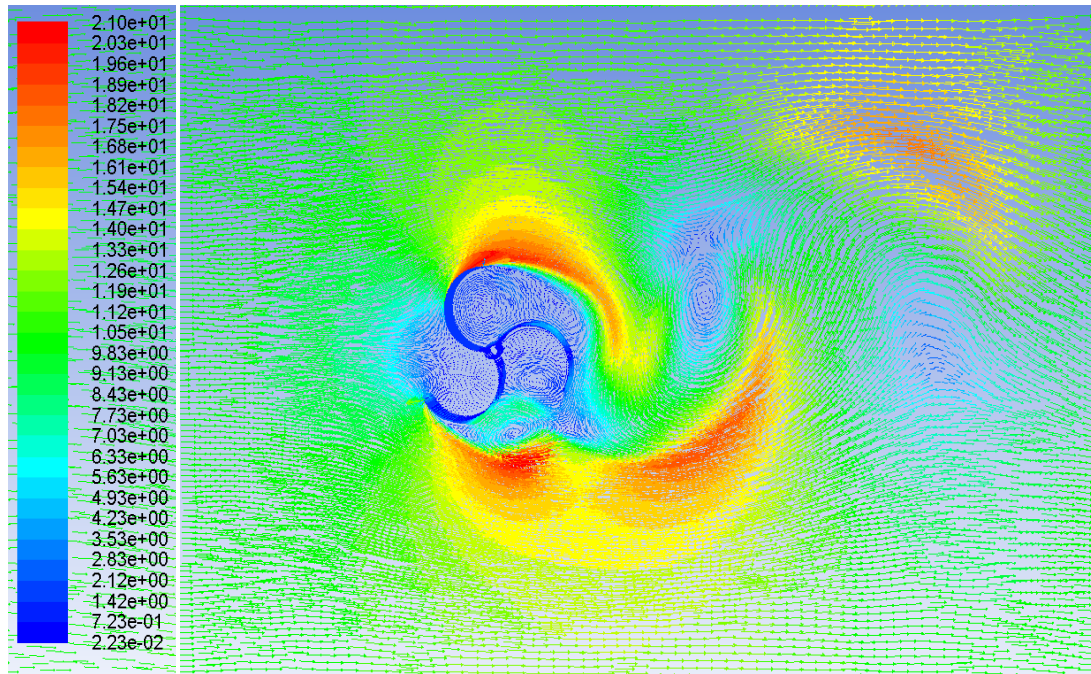


Fig 5.9– 3Blade Turb. 30 Degree orientation- Velocity Vector Display.

Fig 5.9. represents the flow of wind over the turbine blade in the domain. It can be clearly seen that a reverse flow takes place in the area near the turbine blades and also in the wake region. This is shown by filled-arrows which displays the direction in which the wind flows. It can be observed that the air comes from below blade-3 and gets diverted upwards cutting the wake region.

CASE III:3 Blade Turbine- 60 Degree Angle

This case includes a turbine whose blades are positioned at a 60 degree orientation with respect to the direction of the prevailing wind. Along with the boundary conditions rest all other conditions are kept alike CASE I. The meshing scheme of quadrilateral ‘pave’ is applied and the flow model that was used for this case was transition-SST model. Figure 5.10 shows the mesh of the turbine whose blades are oriented at 60 Degree to study the effects of air flow at a certain angle.

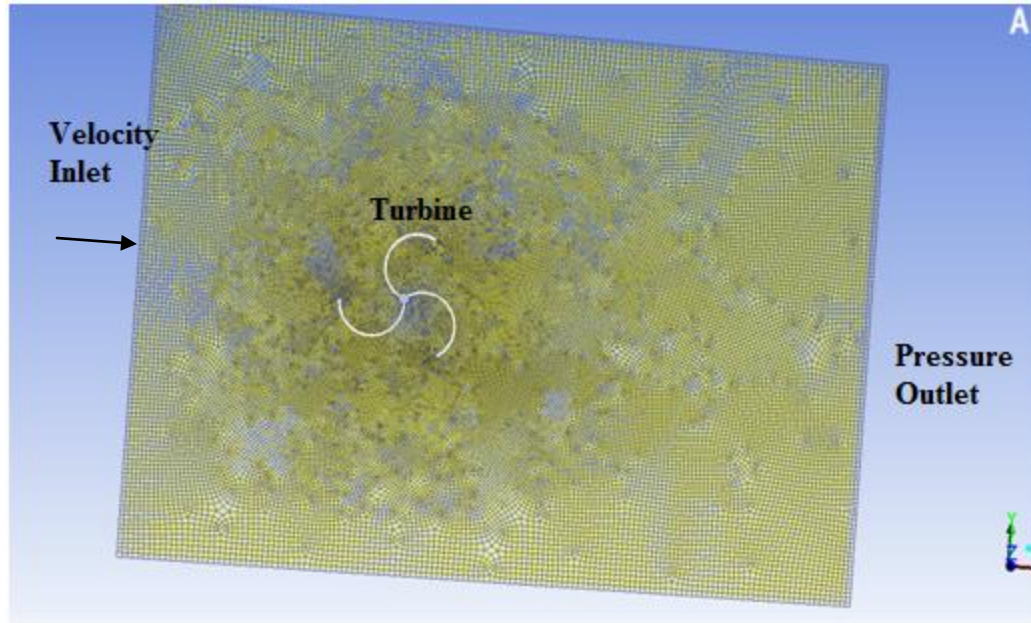


Fig 5.10- Mesh of 3 Blade Turbine at 60 Degree orientation

An input velocity of 10mps was uniformly distributed over the inlet face. The residual criterion was set to a convergence criterion of 10^{-7} for each parameter. The data was monitored after every 50 time steps.

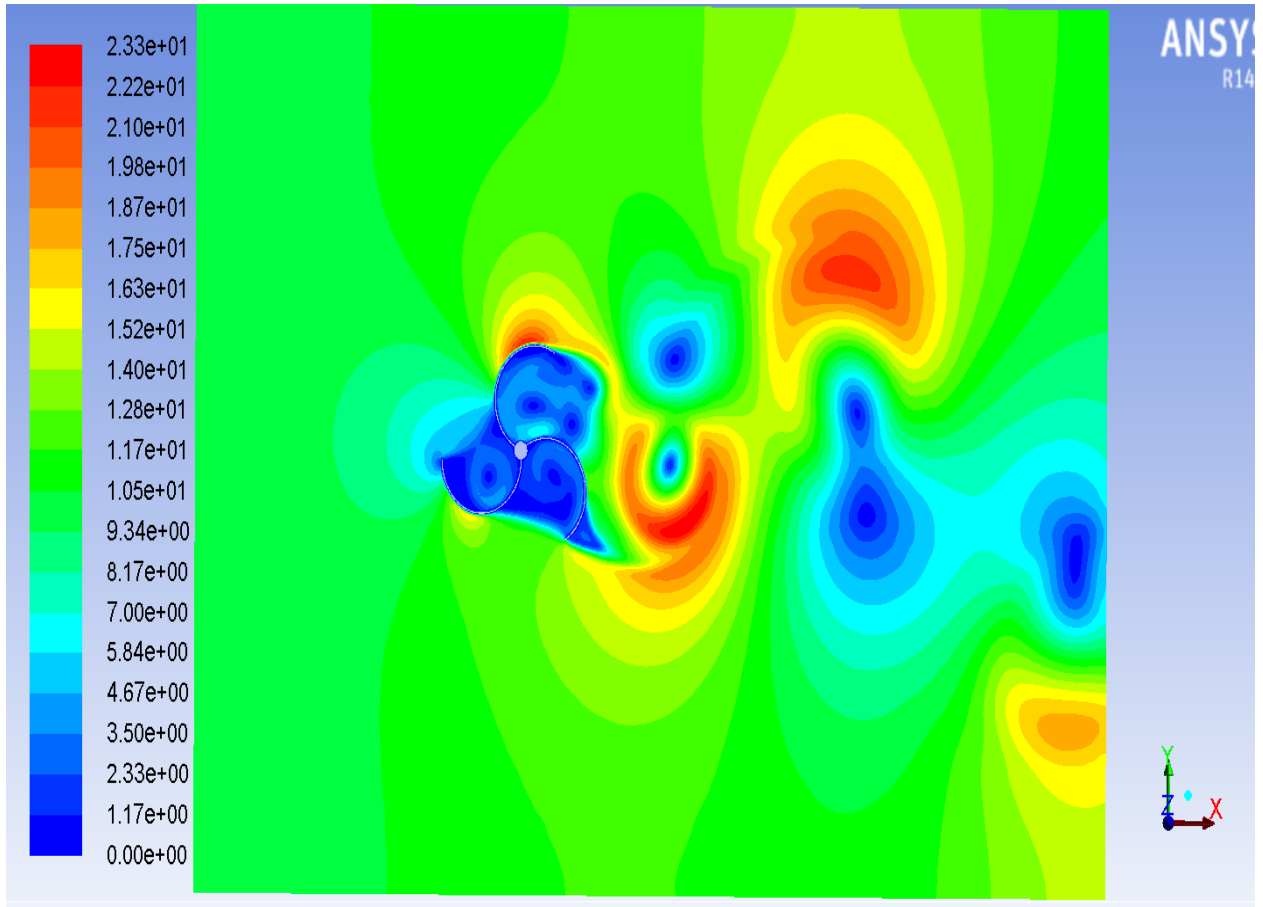


Fig 5.11– 3 Blade Turb. 60 Degree orientation- Velocity Contours , Plane 17'

Figure 5.11 displays the velocity distribution over plane 17'. The value of maximum velocity is 23.35mps which occurs in the close vicinity of blade-1. As the turbine is rotated by 60 degree from its original position, the structure of the wind flow over the turbine has also changed. A high velocity area is produced on the suction side of blade-1. The high velocity area which was produced above blade-1 in CASE II, has shifted downstream (towards output). Also it can be seen that velocity drops to almost zero in some areas to the right side of turbine. This indicates presence of wake region which is surrounded by high velocity belt form top.

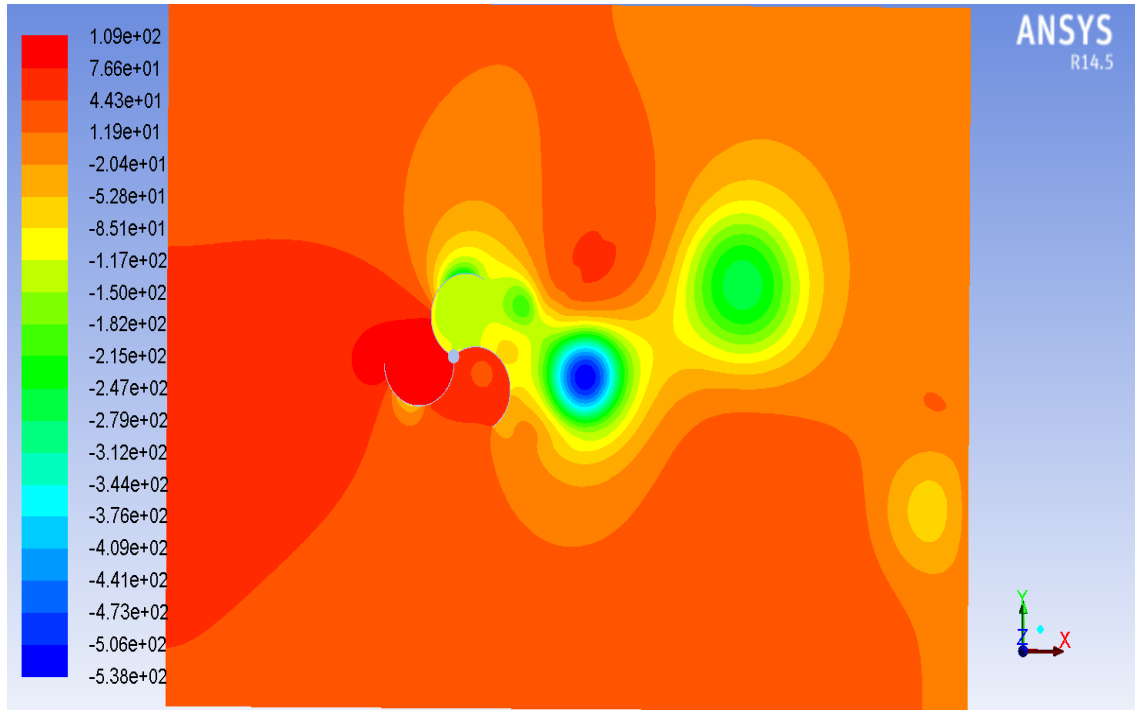


Fig 5.12– 3 Blade Turb. 60 Degree orientation- Static Pressure display, Plane 17

As can be seen from the figure 5.12, the maximum positive pressure (108.97 Pascal) lies in the area between blade-1 and blade-3. The value of maximum negative pressure is -538.00 Pascal which occurs in the wake region, created to the right side of the turbine. The downstream side (Output side) faces negative pressure while the upstream side (Input side) faces positive pressure. Blade-1 developed more force on its pressure side and suction side since each side is facing negative pressure and positive pressure respectively. Observe that the value of negative pressure is much more than those in the previous CASE I and CASE II. The wake region is shifted from above the turbine to right side of the turbine where value of pressure is -538 Pascal.

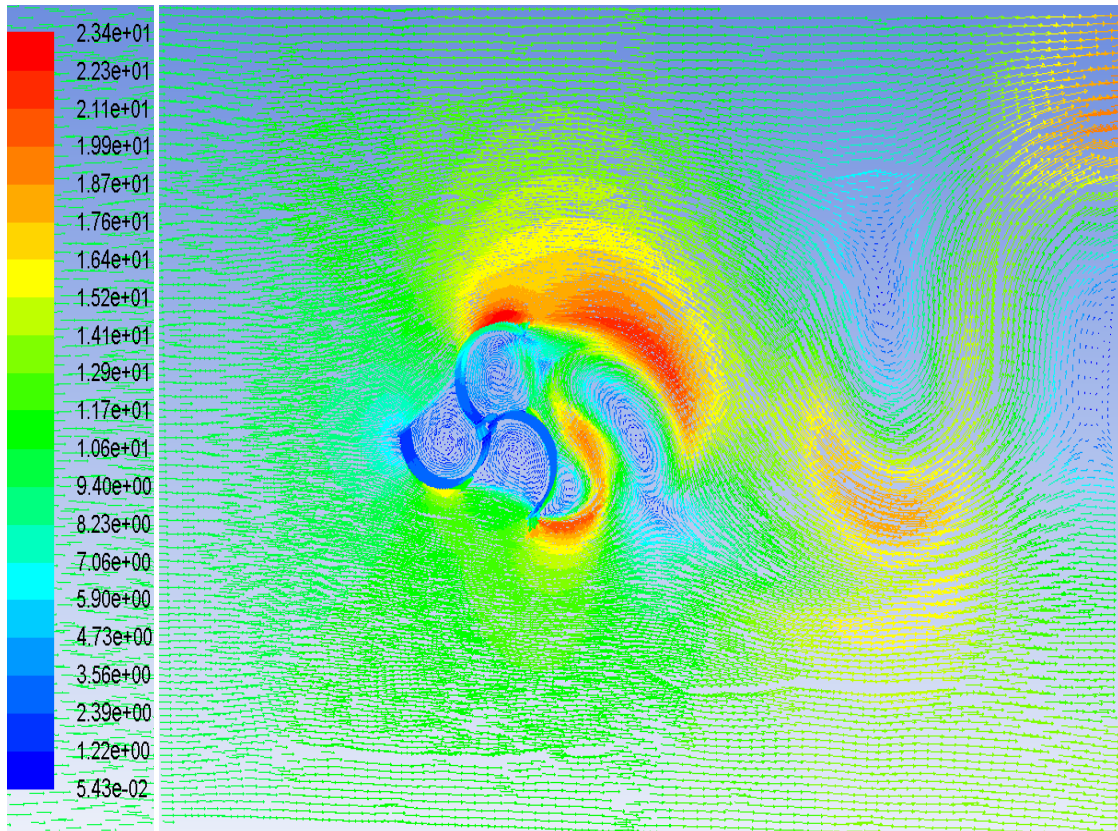


Fig 5.13- 3 Blade Turb- 60 Degree Orientation- Velocity Vector Display Plane 17 [Air Flow over turbine]

The figure 5.13 displays the velocity vectors and the direction in which the flow takes place. The reverse flow takes place in the pressure side of all the three blades. The air flow also gets diverted in a reverse direction in the wake region creating a negative pressure area.

CASE IV:3 Blade Turbine- 90 Degree Angle

This is the fourth and last case picturing a turbine whose blades are positioned at a 90 degree orientation with respect to the direction of the prevailing wind. The boundary conditions remains the same as in CASE I along with the rest of the conditions. The grid

maintains a zone/mesh structure that is similar to that of the previous 3D turbine structured mesh. The meshing scheme of quadrilateral 'pave' was applied and the flow model that was used for this case was transition-SST model. The following fig 5.14 shows the mesh of the turbine whose blades at 90 degree with inlet and outlet shown in blue and red color respectively.

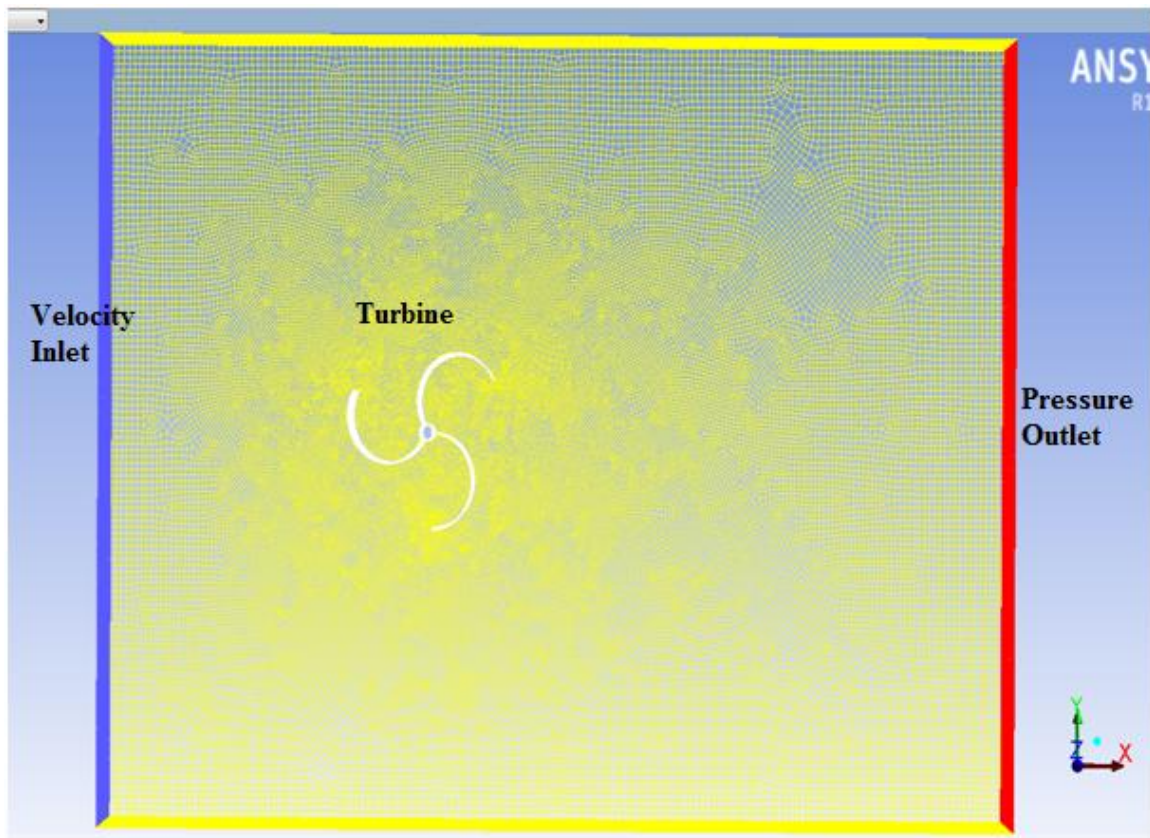


Fig 5.14- Mesh of 3 Blade Turb. at 90 Degree orientation

The input velocity was uniformly distributed about the velocity inlet having a velocity of 10mps. The residual criterion was set to a convergence criterion of 10^{-7} for each parameter. The data was monitored after every 50 time steps.

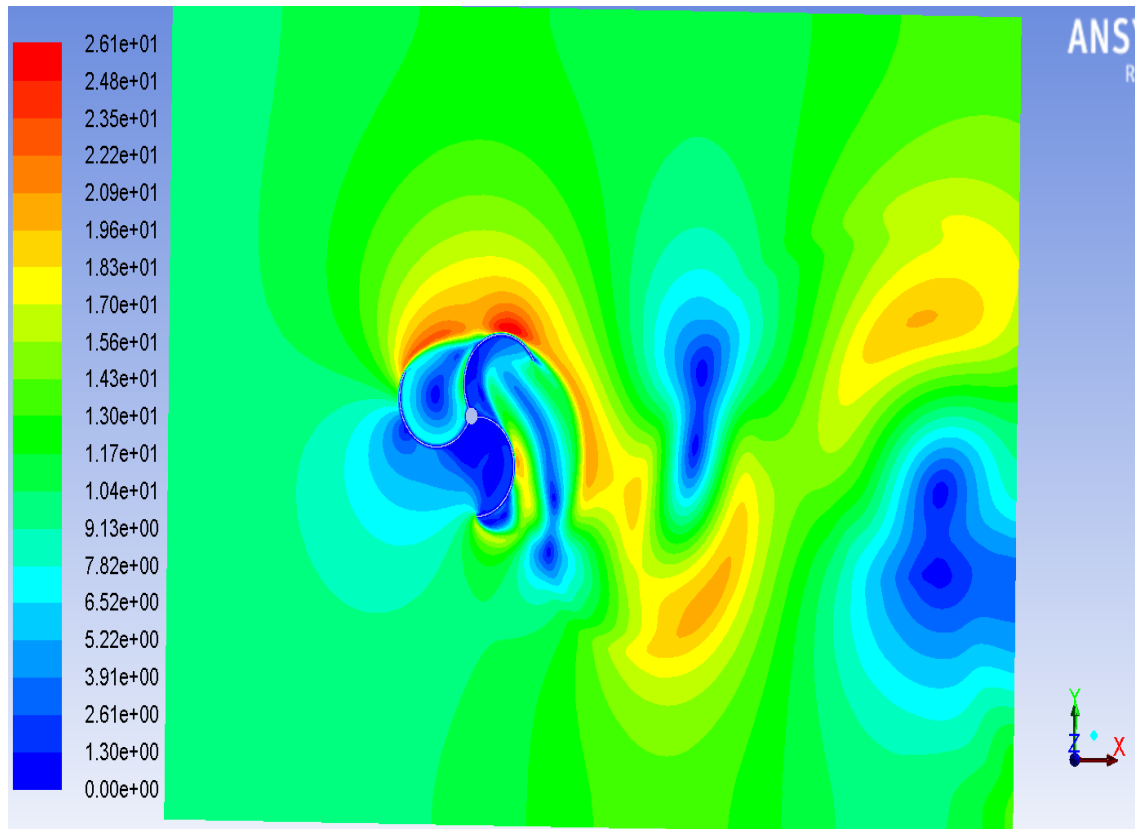


Fig 5.15– 3 Blade Turb. 90 Degree Orientation– Velocity Magnitude, Plane 17'

The figure 5.15 shows the velocity distribution over plane 17' of three blade turbine. The legend in red displays the maximum velocity which has value of around 26.07mps. This velocity appears on the curvature of blade-1 and also at the tip of blade-3. The high velocity area extends from above the turbine to the right side of turbine covering more area on the bottom side and top side near the output face (downstream of the turbine). This indicates a region of high turbulence, thus signifying wake region. Note that the extended area of high velocity does not include the maximum velocity which is 26.07 mps, but it reaches to roughly around 22.2mps. The velocity drops to almost zero in some of the parts in the downstream side.

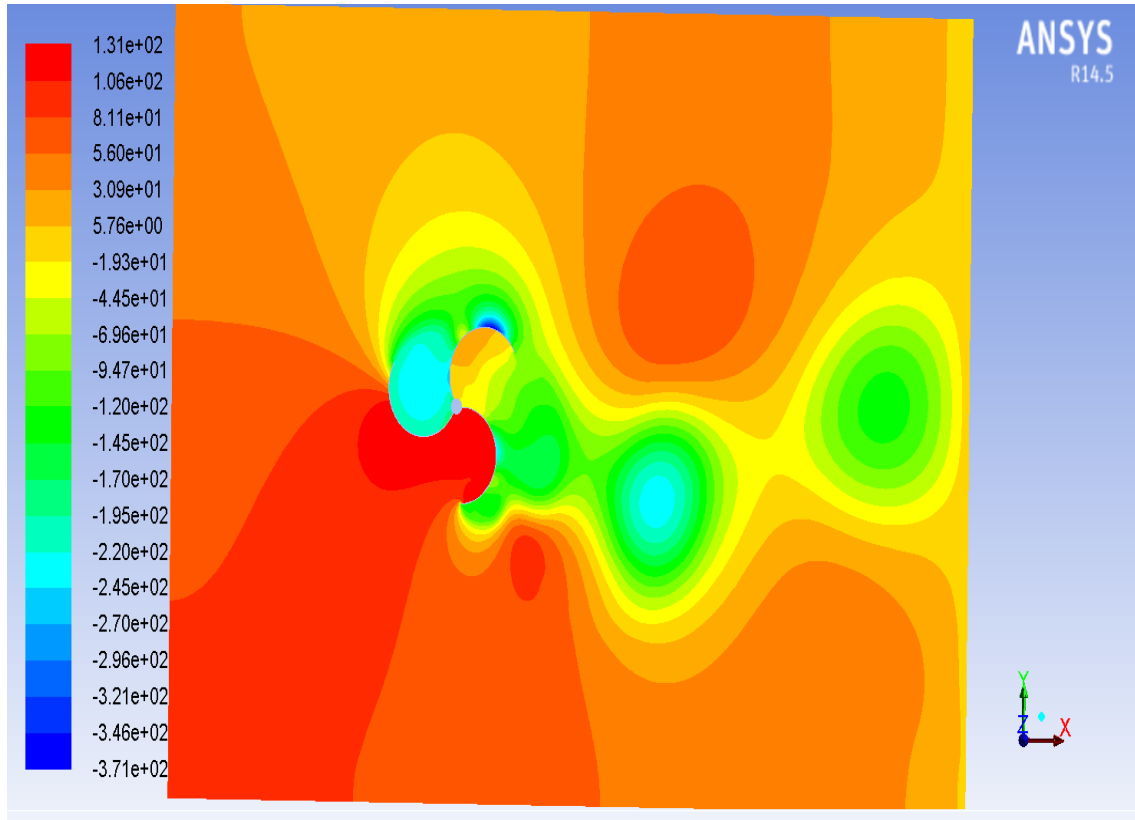


Fig 5.16– 3 Blade Turb. 90 Degree Orientation– Static Pressure, Plane 17'

Figure 5.16 stipulates the distribution of static pressure on plane 17'. The legend in blue indicates maximum negative pressure having a value roughly around $-3.71e+02$ Pascal. This pressure appears on the curvature of blade-1, near the tip of the blade. The area between the blade-1 and blade-3 also faces negative pressure having values roughly around $-2.20e+02$ Pascal. The value of maximum positive pressure is 131.30 Pascal and can be observed in the area between blade-2 and blade-3. Due to the high turbulence the pressure drops in few areas on the downstream side, near the output face. The wake region has pressure drop shown by the legend in light blue (aqua) color on the suction side of blade-2.

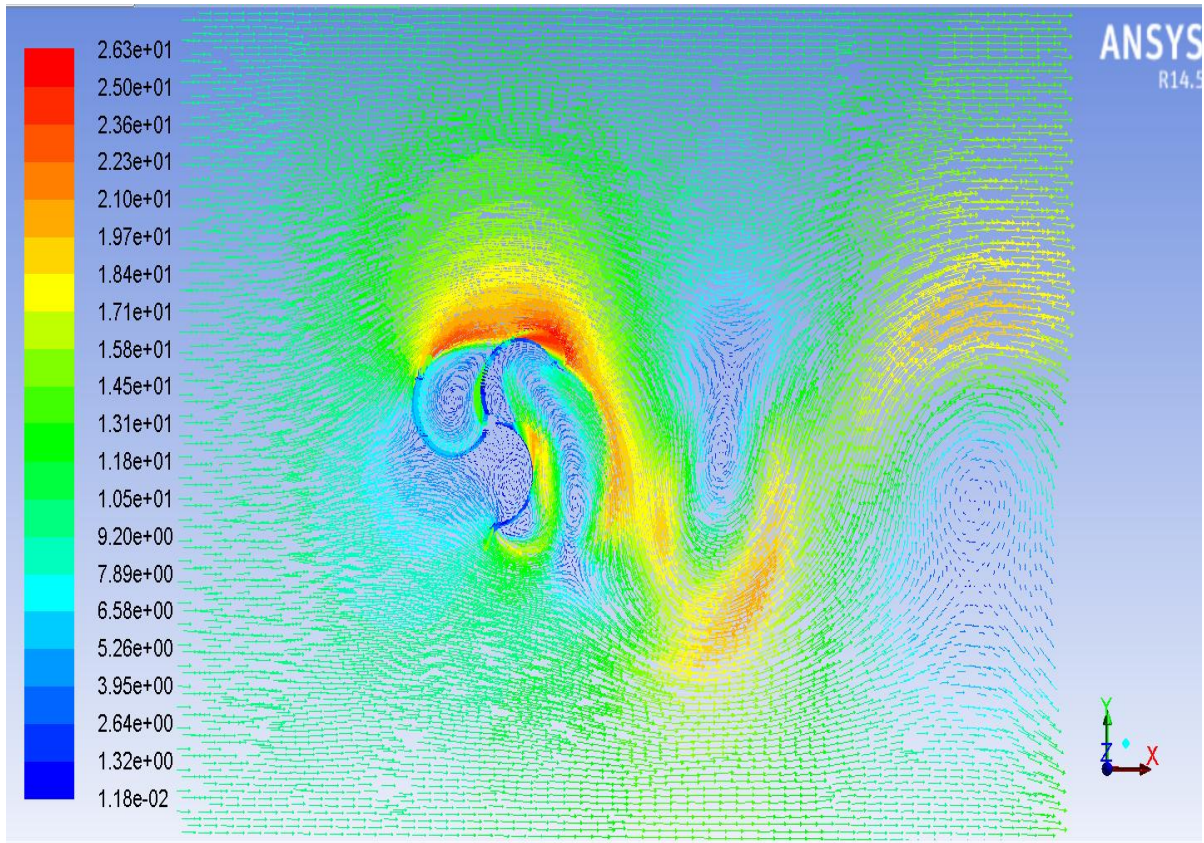


Fig 5.17- 3 Blade Turb.- 90 Degree Orientation- Velocity Vector Display Plane 17' [Air Flow over turbine]

The figure 5.17 displays the flow of air over the turbine on plane 17' in velocity vector form. The velocity vectors are rendered with extensive detail, which gives the user a very clear representation of magnitude and direction on the designated plane. This is extremely important for complex models of reverse flow and vortices are clearly represented. It can be observed that the air flows from above the turbine and advances downwards and again turns upward. Reverse flow can also be observed in wake region.

CHAPTER VI

RESULTS AND CONCLUSION

The basic aim of this thesis, considering cases of 2-Blade and 3-Blade Savonius Wind Turbines, was to study how the two designs are different from each other. So far the turbine was kept steady and its behavior was studied at different angles, keeping the wind velocity constant at 10m/s. It is equally important to study the effects on wind turbine if the velocity varies. Therefore, a study was carried out to demonstrate the effect of wind velocity variations on the turbine performances. Among all the four cases (different angles of wind turbine), only one case was chosen for this purpose which showed maximum change in static pressure and most torque produced on the wind turbine. This study was carried out selecting *case III: 90 Degree Orientation of angle* for Two-Blade Turbine and *case II: 60 Degree Orientation of angle* for Three-Blade Turbine. The different velocities considered were 5m/s, 20m/s, and 30m/s apart from 10m/s which is the standard case. The figures 6.1 and 6.2 display graphs of Force and Torque (produced on turbines) at different Wind velocities.

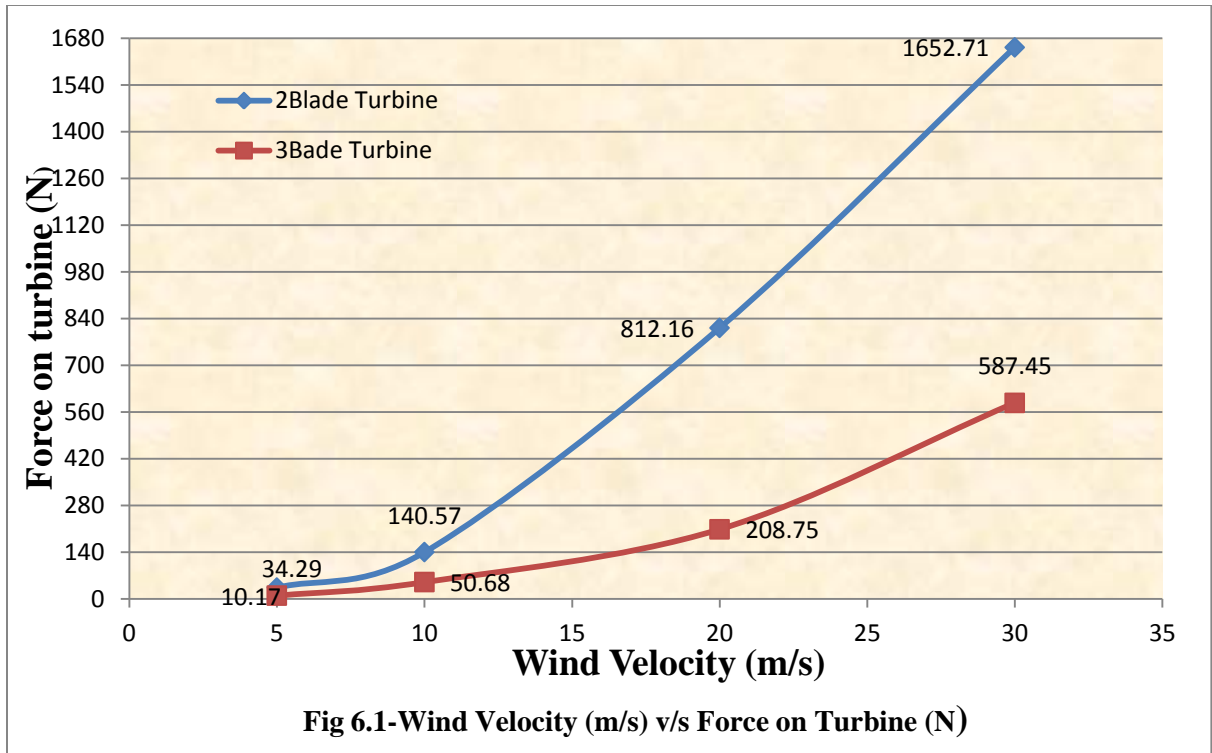


Figure 6.1 is a comparison between Forces generated on 2-Blade wind turbine orientated at 90 Degree and 3-Blade wind turbine orientated at 60 Degree, exposed to different velocities. The graph show difference in Force values for initial values of wind velocity on Y-axis. The graph of 2-Blade turbine shows a drastic increase in force reaching a value of 1652.71 N at a velocity of 30m/s, whereas the force generated on 3-Blade turbine is around 587.45 N. This shows that the blades of 2-Blade turbine are exposed to high forces producing high amount of moments. The figure 6.2 shows comparison of Wind Speed v/s Torque, between 2-Blade and 3-Blade Savonius Wind Turbines.

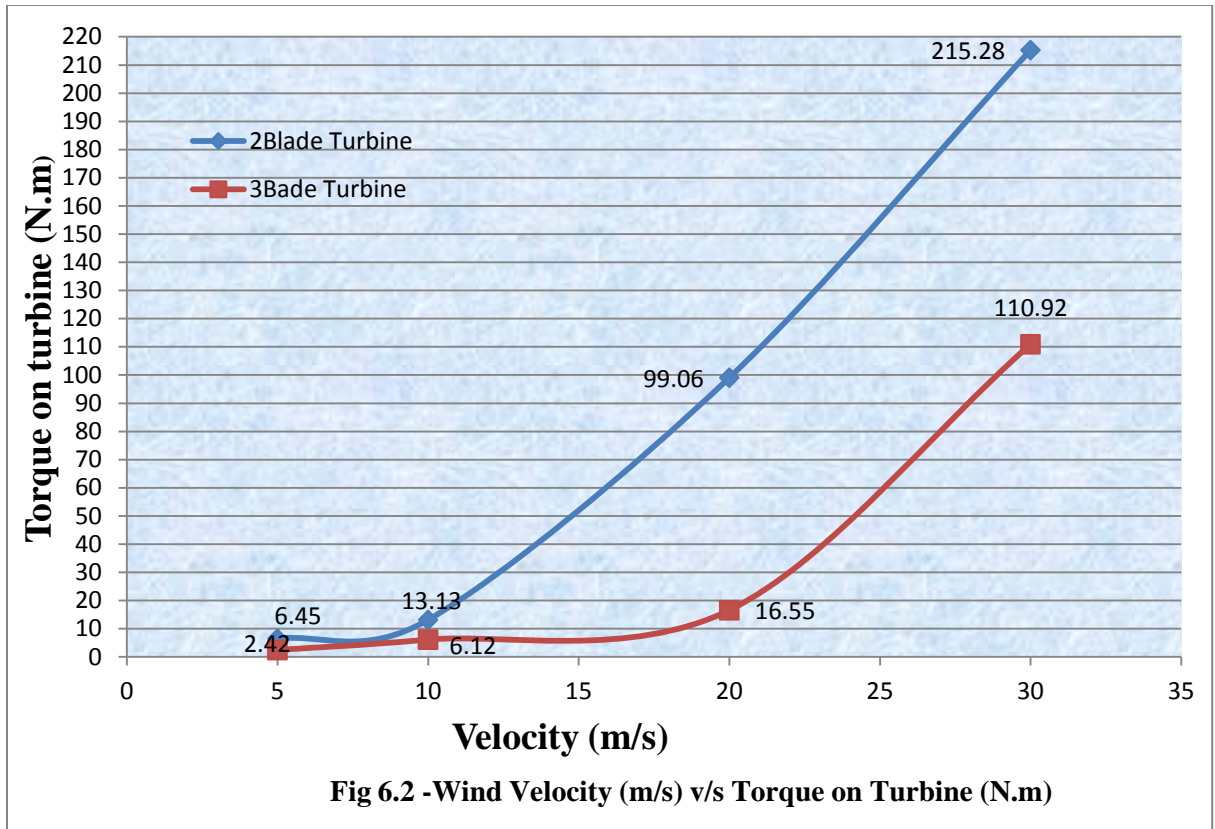
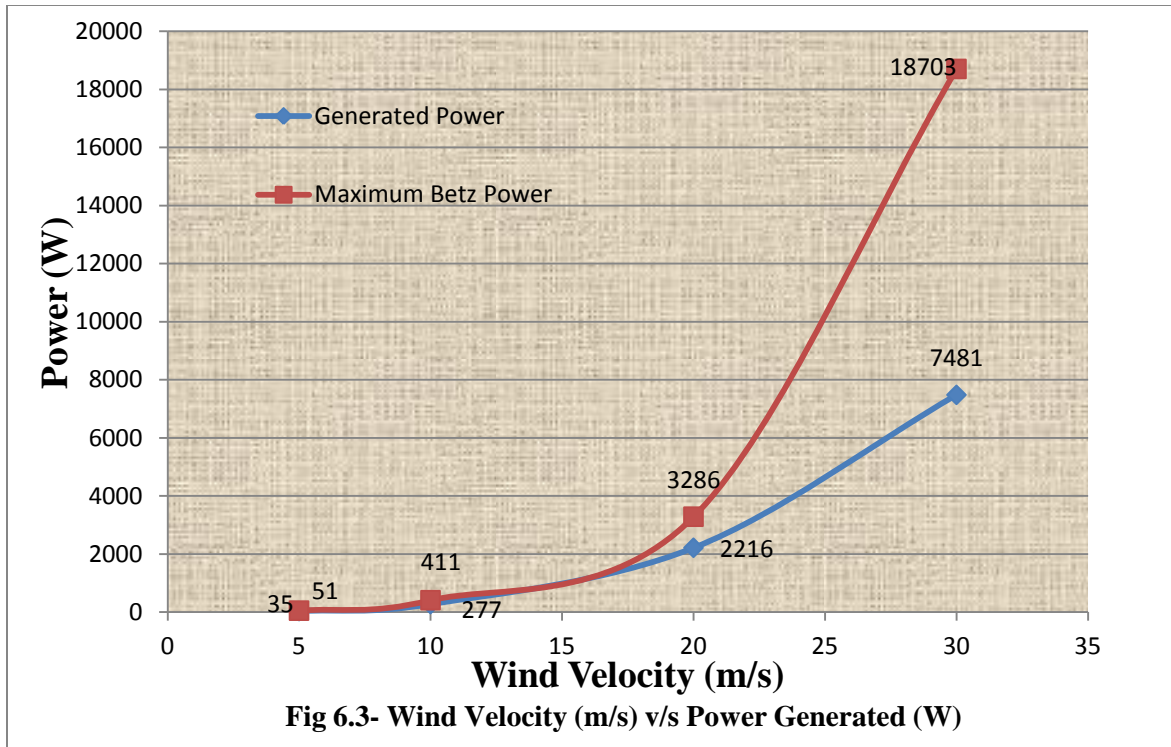


Figure 6.2 displays graph for comparing Torque produced on turbines in response to wind velocity. The graph shows that for the initial velocities (5/s and 10m/s), there is not much difference between the torque values. But for greater velocities 2-Blade Turbine produces higher torque as compared to 3-Blade Turbine. The value of highest torque produced on 3-BT is 110.92Nm while that of 2-BT is 215.28Nm.

The power output of any turbine increases with the increase in wind velocity. The power of wind turbine can be calculated using power formula for wind turbine (Appendix 2).

Figure 6.3 demonstrates the output power generated at different wind velocities.



The figure 6.3 displays a graph comparing available turbine power and Maximum Betz Power. The Betz Limit or Betz Law (Appendix 2) says that-the theoretical maximum power efficiency of any design of wind turbine is 0.59 (i.e. no more than 59% of the energy carried by the wind can be extracted by a wind turbine). As can be seen from the graph 6.3, there is a difference in the generated power and maximum Betz power at wind velocity 35m/s.

6.1 CONCLUSIONS

Figures 6.1, 6.2, and 6.3 shows Forces, Torque and Power produced by 2-Blade Turbine and 3-Blade Turbine and comparison between them. It can be observed that 2-BT produces forces resulting in high amount of torque generation 215.28 Pascal, whereas 3-BT produces torque of amount 110.92 Pascal. Three blade turbines have more stability

due to the extra weight of third blade (due to inertia). Although the third blade results in production of less amount of power, the difference in power generation is not that significant. Maximum change in static pressure occurs when 2-Blade turbine is perpendicular to wind flow direction i.e. at 90 degree and when 3-Blade turbine is at 60 degree orientation with respect to direction of wind flow. As we can see from the Figure 6.3, 2-Blade turbine rotates at higher speed generating more torque than 3-Blade turbine at any given wind velocity.

According to a magazine “Home Power”, two bladed systems generate more power at any given wind speed than three blade systems because they produce more power. But this may result in reduced life span of 2-BT over 3-BT, which may not be worth the initial set up cost, manufacturing cost or even the efficiency produced. Now days, many manufacturers keep an option of both two blade and three blade versions of the same model of turbine. Customers get a chance to select the type of turbine according to their requirement.

The purpose of this thesis was to provide useful information on behavior of wind turbines, from which experts can make informed decisions, and not to make the determination of “best number of bladed turbine”. Experts will need more data for making some projections on future, which cannot be exact. According to me, this is the reason that more additional studies need to be carried out, apart from this work, for complementing the previous experiments and studies. Although Vertical Wind Turbine design needs improvement for reducing initial cost and increasing efficiency, they are a promising and clean way of power/energy generation. This will be a favorable technology in future with proper research and development.

6.2 FUTURE SCOPE

The study conducted provides information on 2-Blade and 3-Blade Vertical Savonius Wind Turbines. There are a number of different analyses which can accompany the results obtained in this thesis. For example, the design of the Savonius wind turbine in this thesis is assumed to be straight (with no curved blades), which could be modified to helical and the same analysis can be carried out. This can allow us to compare different designs for turbines and ultimately provide with a turbine producing more efficiency. In addition, the flow of the turbine can be changed to steady state flow rather than the transient flow assumed in this analysis.

Wind turbines face different velocities throughout the year and hence their capacity to generate power differs constantly. The flow velocity over the turbine is assumed to be 10 m/s in these cases and a few more velocities are considered for comparing the results. But this data is not enough to study the behavior of the turbine since practically the turbine faces different velocities all through the year. Different speeds of wind can be considered producing various results. This can be useful to understand which velocity of wind generates maximum power or is producing stresses in the turbine.

Wind turbine design has a number of aspects like the curvature of blade, weight, surface area and so on which can be optimized to maximize the power generation by putting in some additional efforts. It can be aimed to improve the efficiency of turbines and reliability of the components, along with some structural modifications in the turbine design to capture more percentage of wind.

REFERENCES

1. Althea de Souza. *How to Understand Computational Fluid Dynamics Jargons*. Published: 2005
2. American Wind Energy Association. (2006). *Wind of Web Facts Sheets*. Retrieved October 27, 2006, from American Wind Energy Association.
3. André Bakker. *Applied Computational Fluid Dynamics*. (2006). The Colorful Fluid Mixing Gallery
<http://www.bakker.org/dartmouth06/engs150/05-solv.pdf>
4. Bachu Deb and Rajat Gupta. *Fluid Flow Analysis of Savonius Rotor at Different Rotor Angle Using CFD*. Volume 8 - Number 14 - November 2012 (35-42). ISESCO JOURNAL of Science and Technology.
5. Betz, A. (1996). *Introduction to the Theory of Flow Machines*. Oxford: Pergamon Press.
6. BW van Oudheusden. (2013). *PIV-based pressure measurement*. Published: 7 January, 2013.
<http://iopscience.iop.org/0957-0233/24/3/032001/>
7. Burcin Deda Altan *, Mehmet Atılğan. (2008) *Energy Conversion and Management. (An experimental and numerical study on the improvement of the performance of Savonius wind rotor.)*
Journal homepage: www.elsevier.com/locate/enconman
8. Dennis Cui. *The Sun's the limit*. June 29, 2012. Young Scientist Journal.
<http://www.yjournal.com/article.asp?issn=09746102;year=2012;volume=5;issue=11;spage=6;epage=10;aulast=Cui>

9. F. R. Menter, "Zonal Two Equation k-w Turbulence Models for Aerodynamic Flows," AIAA Paper #93-2906, 24th Fluid Dynamics Conference, July 1993
10. F. R. Menter, "Two-Equation Eddy-Viscosity Turbulence Models for Engineering Applications," AIAA Journal, vol. 32, no. 8, pp. 1598-1605, 1994]
11. Fluent Inc. (2013, January). CFD Flow Modeling Software and Solutions, Online Technical Support Portal. Retrieved January 28, 2013, from Fluent:
http://www.fluent.com/services/technical_support/index.htm
12. Fluent Inc (2001, December). Gambit 2 Tutorial Guide. Lebanon, NH, United States of America.
13. FranciscoToja-Silva, Antonio Colmenar-Santos n, ManuelCastro-Gil. (2013). *Renewable and SustainableEnergyReviews. (Urban wind energy exploitation systems: Behavior under multi directional flow conditions—Opportunities and challenges.)*
Journal homepage: www.elsevier.com/locate/rser
14. Forces on Large Steam Turbine Blades- *RWE npower*. Official Statistics from the UK Energy Company. Retrieved: September 2013 from Forces on Large Steam Turbine Blades.
http://www.raeng.org.uk/education/diploma/maths/pdf/exemplars_advanced/22_blade_forces.pdf
15. Hahm, T., & Kroning, J, (2002). In the Wake of a Wind Turbine. October 2010 form
Fluent: <http://www.fluent.com/about/news/newsletter/02v11i1/a1.htm>

16. Hasnan. *Wind Energy and Wind Power. (Effect of blade number on aerodynamic performance in wind turbine)*. Retrieved August 2013.
<http://winds-energy.blogspot.com/2009/04/effect-of-blade-number-on-aerodynamic.html>
17. Jean-Luc Menet, Nachida Bourabaa. *Increase in the Savonius Rotors Efficiency via a Parametric Investigation*. Retrieved September 2013, from
http://www.wrapwind.com/download/vawt/23_1400_jeanlucmenet_01.pdf
18. Kelley, F. (2002). *Wind Turbine Blade Aerodynamics*. Retrieved October 2006, from
Fluent: <http://www.fluent.com/about/news/newsletters/02v11i1/a2.htm>
19. Kulkarni, A., & Moeykens, S. (2005, January 6). *Flow over a Cylinder*. Retrieved October 2006, from Fluent [Flow Lab 1.2]
20. Magdi Ragheb and Adam M. Ragheb. *Wind Turbines Theory - The Betz Equation and Optimal Rotor Tip Speed Ratio*.
[http://cdn.intechopen.com/pdfs/16242/InTechWind turbines theory the betz equation and optimal rotor tip speed ratio.pdf](http://cdn.intechopen.com/pdfs/16242/InTechWind_turbines_theory_the_betz_equation_and_optimal_rotor_tip_speed_ratio.pdf)
21. Peter J. Schubel * and Richard J. Crossley. *Wind Turbine Blade Design*.
Published: 6 September 2012
www.mdpi.com/journal/energies
22. Masami Sato, and Takaya Kobayashi *A fundamental study of the flow past a circular cylinder using CFD*
http://imechanica.org/files/Sato_MDAC_final_2232012.pdf

23. Rajat Gupta, Ranjan Das, Rituraj, Gautam, Siddhartha Sankar Deka. CFD Analysis of a Two-bucket Savonius Rotor for Various Overlap Conditions. Volume 8 - Number 13 - May 2012 (67-74). ISESCO JOURNAL of Science and Technology.
24. Tannehill, J. C., Anderson, D. A., & Pletcher, R. H. (1997). *Computational Fluid Mechanics and Heat Transfer, Second Edition*. Taylor and Francis.
25. Turbulent Wake Flow behind a Circular Cylinder. Engineering Stuff.
<http://www.eng.fsu.edu/~shih/succeed/cylinder/cylinder.htm>
26. Takaya Kobayashi and Masami Sato. *A fundamental study of the flow past a circular cylinder using Abaqus/CFD*. 2012 Simulia Community Conference.
http://imechanica.org/files/Sato_MDAC_final_2232012.pdf
27. Wind Turbine Power Calculations -RWE npower renewable. Official Statistics from the UK Energy Company. Retrieved: September 2013 from Wind Turbine Power Calculations
http://www.raeng.org.uk/education/diploma/maths/pdf/exemplars_advanced/23_wind_turbine.pdf

APPENDICES

1 GLOSSARY

Algebraic Equations-Equations that need to be solved simultaneously throughout a problem domain in order to find the numerical representations of the problem.

Amplification Factor- This is dimensionless quantity that is used to describe the increase or decrease in flow speed at a given point or over a given region.

$$\text{Amplification Factor} = \frac{\text{velocity of interest}}{\text{Free - stream velocity}}$$

Boundary Layer- For a sufficient large Reynolds number a thin region existed near a solid boundary where viscous effects were at least as important as inertia effects no matter how small the viscosity of the fluid might be.

Boundary Types- are unknown and are often determined in direct correlation with the physical model. Examples of boundary types include- wall, velocity inlet/outlet, pressure inlet/outlet, planes of symmetry.

Case- It is a representation of a physical model that is used to accurately represent and simulate real life engineering situations. Cases are assigned a series of attributes that are specific to a given problem, which so then stored as the variable called 'data'.

CFD- Computational Fluid Dynamics .It is a methodology used to solve complex problems in the field of computational fluid dynamics and heat transfer

Computational Domain - It is often a rectangle but be of any size or shape. Generally through the study of computational fluid dynamics you will need to convert between physical coordinates and transformed coordinates.

Continuum Types- Continuous matter, including both solid/fluids and liquids/gases. Contours- A curve connecting points where the function has a same particular value. IN the instance of wind direction the contour would be classified as an isogon and the wind speed would be classified as an isotach.

Convergence-Solution of the discretized equations tends to the exact solution of the differential equation as the grid spacing tends to zero. Generally if a scheme is consistent and stable, it is convergent.

Coordinate System- A system for assigning a couple of numbers to each point in an n-dimensional space.

Discretization- Concerns the process of transferring continuous models and equations into discrete counterparts. This process is carried out as a first step toward making them suitable for numerical evaluation and implementation on digital computers.

Downstream- Downstream can be defined as the direction of the flows, towards the current of the stream.

External Flow- Flow that does not penetrate the inside of a part or component. Takes place on the external faces of the body given.

Grid/Mesh- Preliminary step to performing the CFD analysis. Discretizes the model and spatial domain into small cells (preferably rectangles of minimum skew, but can consist of pyramidal solids in 3D).

Initialize- The process of specifying initial conditions to a given problem.

Laminar- This flow occurs when a fluid flow in parallel layers with no disruptions between layers. Also called as streamline flow. In fluid dynamics, laminar flow is a flow regime characterized by high momentum diffusion, low momentum convection, and pressure and velocity independence of time.

Map- Regular structured mesh. (Fluent Inc. 2013)

Monitors- categorization of predefined functions that are used to determine when the iterative calculations meet the specified criterion.

Pave- Unstructured Mesh.

PISO- Pressure-Implicit with Splitting of Operations- based on higher degree of approximate relation between corrections for pressure and velocity.

Power Coefficient- The ratio of power produced by a wind energy conversion device to the power in a reference area of the free wind stream. (Energy efficiency and energy renewable-U.S Department of Energy [EERE])

Residual- Residuals are related to the concept of truncation error and are used to determine the proper time to terminate an iterative set of calculations.

Reynolds Number- It is the dimensionless velocity defined as ratio of inertia forces to viscous forces

Turbulent- Turbulence or turbulent flow is a flow regimen characterized by chaotic, stochastic property changes. This includes low momentum diffusion, high momentum convection, and rapid variation of pressure and velocity in space and time.

Submap- Divides an unmapped face into mappable region and then creates a structures mesh in these new regions.

Scheme- An important concept connecting the field of algebraic geometry, commutative algebra and number theory.

Steady- A state that is not affected or influenced by time.)

Streamline- 1) Family of curves that are instantaneously tangent to the velocity vector of the flow. 2) A line everywhere tangent to the velocity vector at a given instant. Note: Streamlines and pathlines are identical in steady flow.

Swept Area-The area (in square feet or meters²) that a wind generator's blades sweep (cover). This is the collector area for a wind generator.

Timeline- is a set of fluid particles that form a line at a given instant.

Transient flow- is flow where the flow velocity and pressure are changing with time.

Tri Primitive- divides a three sided face into three quadrilateral regions and creates a mapped mesh in each region.

Tip speed ratio- is defined as the ratio of the speed of the rotor tip to the free stream wind speed.

$$TSR = \lambda = \frac{\text{speed of rotor tip}}{\text{wind speed}}$$

Unsteady- Differs from steady through the appearance of the term $\rho^*(du/dt)$ in the momentum equation and $d\rho/dt$ in the continuity equation. These equations are also parabolic but with time as the marching parameter.

Upstream - Direction that is opposite the normal direction of the flow, away from the current. (Wikipedia 2013)

Vectors- a concept that is characterized by a magnitude and a direction. Can be one of many attributes such as velocity, pressure, temperature, etc.

Wake Flow/ Wake region- The flow downstream of a body immersed in a stream or the flow behind a body propagating through a fluid. Wakes are narrow elongated regions; filled with large and small eddies.

Wedge Primitive- for a wedge shaped region, creates a triangular mesh at the tip and radial quadrilateral meshes outward. (Fluent Inc. 2013)

2 NOMENCLATURE/ABBREVIATIONS

ρ = density

v = wind velocity

A = swept area of turbine blade

$L=r$ = radius of swept area

P = power output

C_p = Coefficient of power

$P_{generated}$ = power generated (obtained) in this study

k- ϵ model =flow model

transition-SST model= strain separated flow transition model

2BT- Two Blade Turbine

3BT- Three Blade Turbine

FDE- Fluid Dynamic Experiments

GUI - Graphic user interface- is an interface between computer system and user which makes use of mouse pointers, windows and icons.

3 POWER CALCULATIONS AND BETZ LIMIT

The electrical energy generated by wind turbines is obtained by converting wind energy into kinetic rotational wind energy in the turbines and then into electrical energy by generators. The energy generated depends on the wind speed available at the site and swept area of the turbine. The output power of a turbine can be calculated by using the following equation:

$$P = \frac{1}{2}\rho Av \dots \text{eq (1) where:}$$

$$\rho = \text{Air Density} = 1.225 \text{ kg/m}^3$$

$$v = \text{Wind Speed} = 10 \text{ m/s}$$

$$A = \text{Swept Area} = \pi r^2 \text{ (m}^2\text{)} \dots \text{eq (2)}$$

Substituting the value of blade length (l) as the radius (r) of swept area in eq (2) we get:

$$l = r = 24 \text{ inches} = 0.6 \text{ meters}$$

$$A = \pi 0.6^2 = 1.13097 \text{ m}^2$$

Now inserting value of 'A' in eq (1) we get:

$$P = \frac{1}{2} * 1.225 * 1.13097 * 10$$

$$\mathbf{P = 692.71 \text{ W}}$$

A German physicist Albert Betz came to a conclusion that “any conventional (practical) wind turbine cannot convert more than 16/27 (59.3%) of the kinetic energy of the wind into mechanical energy which initiates rotor”. This is known as **BETZ LAW** or **BETZ LIMIT**. This means that any design of wind turbine can produce maximum power efficiency of 0.59 theoretically. This is called “power coefficient” and is given by: $C_p = 0.59$

Now when the Betz limit is considered, the output Power is reduced and the formula becomes:

$$P = \frac{1}{2} \rho A v C_p \qquad P = \frac{1}{2} \rho A v^3 (0.593) \qquad \dots \text{Eq (3)}$$

Now if we consider different velocity speed of the wind for a fix angle of turbine then we get maximum Betz Power for those wind velocities. The following table gives different Betz Power for varying wind velocities.

$P = \frac{1}{2} * 1.225 * 1.13098 * (0.593) * V^3$	Wind Velocity (m/s)	Betz Power Output (W)
	5	51.347
	10	410.78
	20	3286
	30	18703

Table A2-1- Betz Power at varying Wind Velocities

It should be noted that Betz Power is theoretical Power and no wind turbine can operate at this maximum limit. Also value of power coefficient 'Cp' is different for different turbines and it mainly is a function of Wind speed. Practically if all the engineering requirements of a wind turbine are considered, specially its durability and strength, the actual limit of 'Cp' is way below the Betz Limit and lies between 0.35-0.45 for even the best designs of wind turbines. There are some other factors like gearbox, generator, bearings, and friction losses and so on, which again contribute in reducing the Cp and ultimately its power output. It will not be wrong to say that only 10%-30% of kinetic energy is actually converted into and used as electricity. Hence the formula for generated power can be given by:

$$P_{generated} = \frac{1}{2}\rho A v C_p \quad \text{where } C_p \text{ lies between } (0.35-0.45) \quad \dots \text{ Eq (4)}$$

Assuming that the design of wind turbines is good enough, the value of Cp can be assumed to be 0.4. The following table gives different generated Power output for four different velocities.

$P_{generated} = \frac{1}{2} * 1.225 * 1.13098 * (0.4) * V^3$	Wind Velocity (m/s)	Generated Power Output (W)
	5	34.63
	10	277.08
	20	2216
	30	7481

Table A2-2- Generated Power at varying Wind Velocities

It can be observed that generated power from a wind turbine has less value as compared to the theoretical value of Power since the value of power coefficient is lower than the theoretical Cp (Betz Criteria).